# Global Modeling and Assimilation Office

*GMAO Office Note No. 13 (Version 1.0)*

# Soil Moisture Active Passive Mission
# L4_C Data Product Assessment
# (Version 2 Validated Release)

Release Date: 04/29/2016

**Global Modeling and Assimilation Office**
**Earth Sciences Division**
**NASA Goddard Space Flight Center**
**Greenbelt, Maryland 20771**

This page intentionally left blank.

# Soil Moisture Active Passive Mission
# L4_C Data Product Assessment
# (Version 2 Validated Release)

John S. Kimball[1], Lucas A. Jones[1], Joseph Glassy[2],
E. Natasha Stavros[3], Nima Madani[1], Rolf H. Reichle[4],
Thomas Jackson[5], and Andreas Colliander[3]


1 – The University of Montana, Missoula, MT, USA
2 – Lupine Logic, Inc., Missoula, MT, USA
3 – NASA Jet Propulsion Laboratory, Pasadena, CA, USA
4 – NASA Goddard Space Flight Center, Greenbelt, MD, USA
5 – USDA Agricultural Research Service, Beltsville, MD, USA

Document maintained by Rolf Reichle (GMAO)

Approved by:


_____

Steven Pawson                          Date

Head, Global Modeling and Assimilation Office
Code 610.1, NASA GSFC

**REVISION HISTORY**

| Revision | Date | Sections Changed | Reason for Change |
|---|---|---|---|
| Initial Version 1.0 | 4/21/2016 | All | Initial Document |

# TABLE OF CONTENTS

# 1 EXECUTIVE SUMMARY

The SMAP satellite was successfully launched January 31st 2015, and began acquiring Earth observation data following in-orbit sensor calibration. Global data products derived from the SMAP L-band microwave measurements include Level 1 calibrated and geolocated radiometric brightness temperatures, Level 2/3 surface soil moisture and freeze/thaw geophysical retrievals mapped to a fixed Earth grid, and model enhanced Level 4 data products for surface to root zone soil moisture and terrestrial carbon ($CO_2$) fluxes. The post-launch SMAP mission Cal/Val Phase had two primary objectives for each science product team: 1) calibrate, verify, and improve the performance of the science algorithms, and 2) validate accuracies of the science data products as specified in the L1 science requirements. This report provides analysis and assessment of the SMAP Level 4 Carbon (L4_C) product pertaining to the validated release. The L4_C validated product release effectively replaces an earlier L4_C beta-product release (Kimball et al. 2015). The validated release described in this report incorporates a longer data record and benefits from algorithm and Cal/Val refinements acquired during the SMAP post-launch Cal/Val intensive period.

The SMAP L4_C algorithms utilize a terrestrial carbon flux model informed by SMAP soil moisture inputs along with optical remote sensing (e.g. MODIS) vegetation indices and other ancillary biophysical data to estimate global daily net ecosystem $CO_2$ exchange (NEE) and component carbon fluxes for vegetation gross primary production (GPP) and ecosystem respiration ($R_{eco}$). Other L4_C product elements include surface (<10 cm depth) soil organic carbon (SOC) stocks and associated environmental constraints to these processes, including soil moisture and landscape freeze/thaw (FT) controls on GPP and respiration (Kimball et al. 2012). The L4_C product encapsulates SMAP carbon cycle science objectives by: 1) providing a direct link between terrestrial carbon fluxes and underlying FT and soil moisture constraints to these processes, 2) documenting primary connections between terrestrial water, energy and carbon cycles, and 3) improving understanding of terrestrial carbon sink activity in northern ecosystems.

There are no L1 science requirements for the L4_C product; however self-imposed requirements have been established focusing on NEE as the primary product field for validation, and on demonstrating L4_C accuracy and success in meeting product science requirements (Jackson et al. 2012). The other L4_C product fields also have strong utility for carbon science applications; however, analysis of these other fields is considered secondary relative to primary validation activities focusing on NEE. The L4_C targeted accuracy requirements are to meet or exceed a mean unbiased accuracy (ubRMSE) for NEE of 1.6 g C m$^{-2}$ d$^{-1}$ or 30 g C m$^{-2}$ yr$^{-1}$, emphasizing northern (≥45°N) boreal and arctic ecosystems; this is similar to the estimated accuracy level of *in situ* tower eddy covariance measurement-based observations (Baldocchi 2008).

Methods used for L4_C performance and validation assessments include: 1) qualitative evaluations of product fields in relation to characteristic spatial and seasonal patterns; 2) comparisons of daily carbon flux estimates with *in situ* tower eddy covariance measurement-based daily carbon flux observations from core tower validation sites [CVS]; 3) comparisons of daily carbon flux estimates with more extensive historical tower carbon flux observations from global FLUXNET data archives; and 4) consistency checks against other synergistic global carbon products, including soil carbon inventory records, satellite-based productivity (GPP) records, global GPP records derived from tower observation upscaling methods, and satellite-based observations of solar induced canopy fluorescence (SIF) as a surrogate for net photosynthesis and GPP. The above CVS comparisons involve approximately 26 individual tower sites; 10 of these sites emphasize northern (≥45°N) ecosystems, which are a primary focus of the L4_C product science objectives, while 16 sites represent a diverse range of other global biome types. The CVS comparisons involve active participation from SMAP tower validation partners who have agreed to contribute near real-time tower observation data records. A larger set of historical tower observation records from 228 globally distributed sites was also used for L4_C validation and was provided by the FLUXNET La Thuile tower data synthesis (Baldocchi 2008); these data extend over multiple (2-7) years

and were used to establish climatological records for each site, including daily means and variability (standard deviation, SD). The above analyses build upon an earlier L4_C beta release and product validation assessment (Kimball et al. 2015) and exceed criteria established by the Committee on Earth Observing Satellites (CEOS) for Stage 1 validation based on a limited set of core validation sites. These activities also satisfy criteria for Stage 2 validation through expanded regional and global assessments involving a diverse set of independent observations. The above activities also approach Stage 3 requirements by including detailed characterization and quantification of product uncertainties in relation to a diverse set of globally representative reference data encompassing a nearly complete annual cycle of SMAP observations.

The primary methods and metrics used for the L4_C Cal/Val assessment include comparisons of collocated time series plots of tower observations with L4_C daily outputs. Comparisons involving CVS sites are both spatially and temporally consistent, while comparisons using the more extensive FLUXNET tower site records are spatially but not temporally consistent as they involve product evaluations against historical tower observations. Other methods employed for L4_C evaluations include qualitative comparisons of latitudinal means and spatial distributions between L4_C outputs and similar spatially contiguous climatological variables derived from other independent satellite, inventory and model-based products. Metrics used to evaluate relative agreement between L4_C product fields and the independent observations include Pearson correlation (R), RMSE differences, unbiased RMSE differences (ubRMSE; defined here as the residual variance of a least squares fit between observed and estimated quantities intended to quantify the random, as opposed to systematic, error), bias and model sensitivity diagnostics. The metrics used to evaluate L4_C NEE correspondence and target accuracy requirements for product success primarily focus on bias-adjusted (primary) results, but also include secondary assessments of the unadjusted results.

This report notes limitations in the current L4_C validated-release product, including the use of: 1) SMAP L4_SM Nature Run (NRv4) soil moisture inputs for carbon model initialization and calibration, and 2) GEOS-5 surface temperatures to define FT controls on estimated carbon fluxes rather than SMAP observations. These limitations will be addressed in a future L4_C product release. Nevertheless, the current L4_C validated release benefits from globally extensive validation activities, more detailed product performance metrics, a longer operational data record and associated calibration refinements relative to an earlier beta-release product (Kimball et al. 2015). The L4_C validated-release effectively replaces the beta-release product and has sufficient maturity, quality and precision to support science level investigations.

# 2   OBJECTIVES OF CAL/VAL

During the post-launch SMAP mission Cal/Val (Calibration/Validation) intensive Phase there were two objectives for each science product team:

- Calibrate, verify, and improve the performance of the science algorithms, and
- Validate accuracies of the science data products as specified in the Level 1 (L1) science requirements according to the Cal/Val timeline.

This process is illustrated in **Figure 2.1**. In this Assessment Report the progress of the L4_C team in addressing these objectives for validated release is described. The approaches and procedures utilized follow those described in the SMAP Cal/Val Plan [Jackson et al. 2012] and Algorithm Theoretical Basis Document for the Level 4 Carbon Data Product [Kimball et al. 2012].
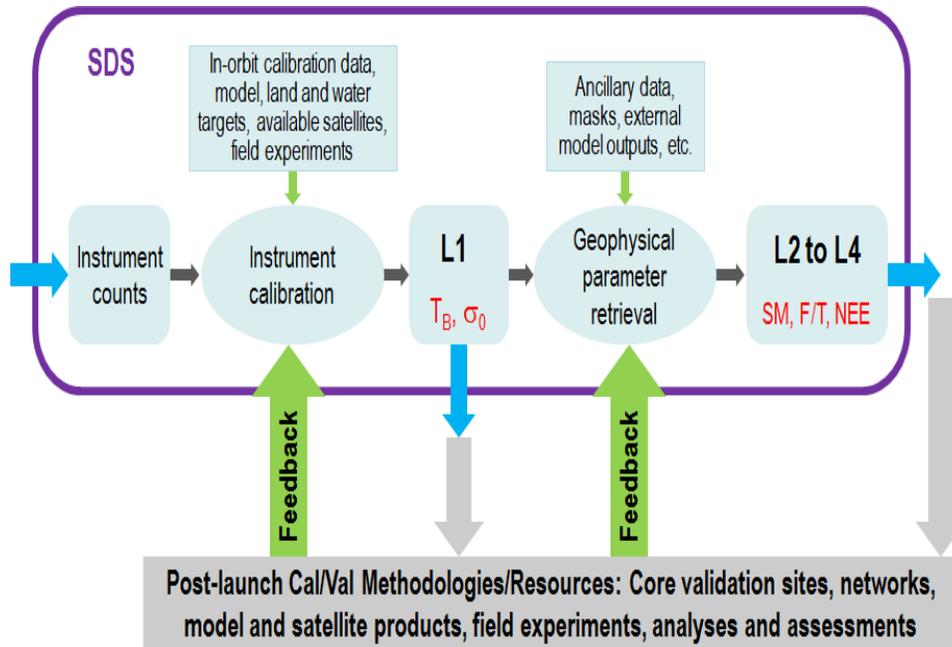
**Figure 2.1**. Overview of the SMAP Cal/Val Process.

SMAP established a unified definition base in order to effectively address the mission requirements. These are documented in the SMAP Handbook/ Science Terms and Definitions [Entekhabi et al. 2014], where Calibration and Validation are defined as follows:

- *Calibration*: The set of operations that establish, under specified conditions, the relationship between sets of values or quantities indicated by a measuring instrument or measuring system and the corresponding values realized by standards.
- *Validation:* The process of assessing by independent means the quality of the data products derived from the system outputs.

The L4_C product does not have a documented L1 accuracy requirement; instead the L4_C team adopted a self-imposed accuracy requirement threshold of 1.6 g C m$^{-2}$ d$^{-1}$ or 30 g C m$^{-2}$ yr$^{-1}$ (RMSE) for the mean bias-adjusted model NEE outputs, emphasizing northern ($\geq$45°N) ecosystems, and at the level of observation uncertainty from tower eddy covariance monitoring sites (Baldocchi 2008).

The L4_C validated release represents a significant upgrade of an earlier beta release product version (Kimball et al. 2015). In assessing the maturity of the L4_C product, the L4_C team considered guidelines from the Committee on Earth Observation Satellites (CEOS) Working Group on Calibration and Validation (WGCV):

- Stage 1: Product accuracy is assessed from a small (typically < 30) set of locations and time periods by comparison with *in situ* or other suitable reference data.
- Stage 2: Product accuracy is estimated over a significant set of locations and time periods by comparison with reference *in situ* or other suitable reference data. Spatial and temporal consistency of the product and with similar products has been evaluated over globally representative locations and time periods. Results are published in the peer-reviewed literature.
- Stage 3: Uncertainties in the product and its associated structure are well quantified from comparison with reference *in situ* or other suitable reference data. Uncertainties are characterized in a statistically robust way over multiple locations and time periods representing global

conditions.  Spatial and temporal consistency of the product and with similar products has been evaluated over globally representative locations and periods.  Results are published in the peer-reviewed literature.

- Stage 4: Validation results for stage 3 are systematically updated when new product versions are released and as the time-series expands.

For the L4_C validated release, Stage 1 and Stage 2 (global assessment) criteria have been met and are relatively mature, and progressing into Stage 3 activities.  Future product releases will benefit from ongoing Cal/Val program activities involving longer data records and periodic algorithm and data calibration refinements and updates. These activities will continue through all Cal/Val stages over the SMAP mission life span.

# 3   EXPECTED L4_C ALGORITHM AND PRODUCT PERFORMANCE

The L4_C algorithm performance, including variance and uncertainty estimates of model outputs, was determined during the mission pre-launch phase through spatially explicit model sensitivity studies using available model inputs similar to those currently being used for operational production and evaluating the resulting model simulations over the observed range of northern ($\geq 45$ °N) and global conditions (Kimball et al. 2012, Entekhabi et al. 2014). The L4_C algorithm options were also evaluated during the mission prelaunch phase, including deriving canopy fPAR (fraction of photosynthetically active radiation absorbed by the canopy) from lower order NDVI (Normalized Difference Vegetation Index) inputs in lieu of using MODIS (MOD15) fPAR; and including an explicit model representation of boreal fire disturbance recovery impacts. These results indicated that the L4_C accuracy requirements (i.e. NEE RMSE $\leq 30$ g C m$^{-2}$ yr$^{-1}$) could be met from the baseline algorithms over more than 82% and 89% of global and northern vegetated land areas, respectively (Yi et al. 2013, Kimball et al. 2012).

The global L4_C algorithm error budget for NEE derived during the mission prelaunch phase indicated that the estimated NEE RMSE uncertainty is proportional to GPP and is therefore larger in higher biomass productivity areas, including forests and croplands. Likewise, NEE RMSE uncertainty is expected to be lower in less productive areas, including grasslands and shrublands. Expected model NEE RMSE levels were also generally within targeted accuracy levels (NEE RMSE $\leq 30$ g C m$^{-2}$ yr$^{-1}$) for characteristically less productive boreal and Arctic biomes. The estimated NEE uncertainty was lower than expected in some warmer tropical high biomass productivity areas (e.g. Amazon rainforest) because of reduced low temperature and moisture constraints to the L4_C respiration calculations so that the bulk of model uncertainty is contributed by GPP in these areas. Model NEE uncertainty in the African Congo was estimated to be relatively larger than in Amazonia due to drier climate conditions in central Africa and associated larger uncertainty contributions of soil moisture and temperature inputs to the model respiration and GPP calculations.

# 4   L4_C PROCESSING OPTIONS

The L4_C validated-release product incorporates two primary processing options that are implemented in the algorithm preprocessing stage for handling of the daily model inputs. These processing options are distinct from other options that are more internal to the model algorithms (Kimball et al. 2012). The major preprocessing options used in the L4_C validated-release include the use of: 1) estimated clear-sky fPAR for missing or lower quality MODIS fPAR inputs, and 2) GMAO surface temperature fields to estimate frozen temperature constraints to the GPP calculations instead of SMAP FT defined constraints. The use

of these preprocessing options are noted in the L4_C product bit flags as defined in the product specification document (Glassy et al. 2015).

The preprocessing options used in the validated-release product include a grid cell-wise selection of a MODIS fPAR 8-day climatology value where data quality flag information from the operational MODIS fPAR inputs indicate missing or lower quality (QC) cloud contaminated data. The static MODIS global fPAR climatology is part of the ancillary data used for L4_C processing and was derived on a per grid-cell basis as the mean fPAR value for each 8-day time step over an annual cycle as determined from the best QC MODIS MOD15 fPAR long-term (2000-2012) record. The spatial extent of the global MODIS fPAR climatology also defines the global L4_C product domain. The use of the fPAR screening process and climatology generally improves model performance, especially in areas with persistent cloud cover, including the tropics and boreal/Arctic ecosystems. However, frequent substitution of current fPAR retrievals for alternative climatological values established from a long-term historical record may degrade model sensitivity to seasonal and annual climate variations, impacts for recent climate trends and extreme events, and recent land use and land cover changes. The fPAR quality bit flag information in the L4_C product provides a record of the spatial distribution and temporal frequency of these substitutions and facilitates future studies to evaluate these impacts.

The L4_C validated product release includes the use of a land surface temperature based FT frozen flag to define frozen temperature constraints to the model GPP calculations (Kimball et al. 2012); here daily surface temperature inputs from the GMAO GEOS-5 land model are used to define the FT flag, where temperatures below a 0.0°C threshold are defined as frozen. The FT flag was originally intended to be defined from SMAP radar FT retrievals derived at 3-km spatial resolution, but this approach was discarded following the SMAP radar instrument failure. The major impact of using temperature-defined frozen flags from the land model is that the FT flags are derived from relatively coarse simulations that are not directly informed by SMAP observations. The current use of temperature based FT frozen flag information in the L4_C calculations is expected to have the greatest impact in northern ecosystems with greater frequency of frozen conditions, and in complex terrain and during seasonal FT transitions with larger FT spatial heterogeneity (Du et al. 2015; Podest et al. 2014). Future L4_C product releases will incorporate Cal/Val refinements using SMAP passive microwave sensor-based freeze-thaw (FT) information having enhanced L-band sensitivity to landscape FT dynamics.

# 5   APPROACH FOR L4_C CAL/VAL: METHODOLOGIES

Validation is critical for accurate and credible product usage and must be based on quantitative estimates of uncertainty.  For satellite-based observations, validation should include direct comparison with independent correlative measurements.  The assessment of uncertainty must also be conducted and presented to the community in normally used metrics in order to facilitate acceptance and implementation.

During the mission definition and development period, the SMAP Science Team and Cal/Val Working Group identified the metrics and methodologies that would be used for L2-L4 product assessment.  These metrics and methodologies were vetted in community Cal/Val Workshops and tested in SMAP pre-launch Cal/Val rehearsal campaigns.  The methodological elements identified and their general roles are:

1. Core Validation Sites: Accurate estimates of products at matching scales for a limited set of conditions
2. Sparse Networks: One point in the grid cell for a wide range of conditions
3. Satellite Products: Estimates over a very wide range of conditions at matching scales
4. Model Products: Estimates over a very wide range of conditions at matching scales
5. Field Campaigns: Detailed estimates for a very limited set of conditions

In the case of the L4_C data product, all of the above elements can contribute to product assessment and improvement. With regard to the CEOS Cal/Val stages, Core Validation Sites address Stage 1 and Satellite and Model Products are used for Stage 2 and beyond. Sparse Networks fall between these two stages. The above methodological elements 1-4 were engaged in preparation for both the L4_C beta-release (Kimball et al. 2015) and validated product release. The primary differences between the validated and beta release assessments are the length of operational data record evaluated, the level of maturity and calibration refinement of the model algorithms and inputs, and maturity of the product format.

# 6  PROCESS USED FOR VALIDATED RELEASE

In order to meet requirements for a May 2016 L4 product validated-release, the SMAP L4_C team generally confined the product assessment to the initial 11 month operational record extending between April, 2015 and February, 2016. The assessment period represents a nearly complete annual cycle of observations, capturing the global pattern and seasonal cycle of terrestrial carbon fluxes and underlying environmental controls for the initial year of SMAP observations. Future product updates will involve a longer observational data record, allowing detailed assessments of inter-annual variability in these processes, while benefiting from continuing algorithm and product calibration improvements and refinements.

Frequent product performance and validation assessments were conducted over the initial record using tower eddy covariance measurement-based daily $CO_2$ flux observations from up to 26 participating CVS tower sites. The periods of record of the tower observations used for the CVS comparisons varied due to differences in measurement records, data quality and formatting, and the timing of data submissions from individual tower partners. These comparisons involved spatially and temporally collocated daily tower observations and L4_C product outputs emphasizing NEE and GPP variables. Tower measurement based estimates of daily ecosystem respiration ($R_{eco}$) were also used to evaluate L4_C product based $R_{eco}$ estimates derived as the daily difference between NEE and GPP. Model performance was also evaluated against daily climatologies of the estimated carbon variables derived from long-term (2000-2013) MODIS fPAR and GEOS-5 (SMAP NRv4) surface meteorology records. The CVS comparisons involved periodic teleconferences with the participating tower PIs to solicit local expertise in evaluating and interpreting product results in context with the tower observations and associated uncertainty.

In addition to the CVS comparisons, model and product performance was evaluated using more extensive historical daily tower observations from 228 globally distributed sites represented by the FLUXNET La Thuille synthesis dataset (Baldocchi 2008). The unbiased RMSE performance of L4_C model estimated NEE and component carbon fluxes was evaluated against the range of observed variability in carbon fluxes over the global domain and within the major plant functional type (PFT) classes represented by multi-year tower observational records spanning a large global range of vegetation and climate conditions.

The L4_C assessment activities included consistency checks against similar carbon variables available from other independent global data products, including the MODIS (Collection 5) MOD17A2 GPP record (Zhao and Running, 2010) and the MPI-MTE global GPP record (Jung et al. 2011). A global monthly composited SIF (solar-induced canopy fluorescence) observation record derived from the ESA GOME-2 sensor (Joiner et al. 2013) was also used as a GPP proxy for evaluating estimated global patterns and latitudinal gradients in the L4_C GPP calculations. The L4_C NEE results were also compared against GFED-CASA optimized global land biospheric carbon fluxes from the NOAA ESRL CarbonTracker (CT2013B) atmospheric transport model inversion framework (Peters et al. 2007).

The L4_C validated-release incorporates a longer data record and the latest model and product calibration refinements, effectively replacing an earlier beta-release product version (Kimball et al. 2015).

The L4_C validated-release was determined to meet a minimum set of satisfactory model and product performance metrics, involving: 1) demonstrations that the L4_C product outputs are consistent with known global and seasonal patterns, and that the magnitudes of estimated carbon fluxes are within realistic ranges for the major global PFT classes represented; 2) demonstrations that model performance is within design specifications, with no apparent model errors or anomalies. The results of these product assessments are summarized below.

# 7   ASSESSMENTS

## 7.1   Global Patterns and Features

General global patterns and seasonal dynamics of the major L4_C product fields were evaluated in addition to more robust quantitative assessments of product performance and accuracy. These qualitative assessments were used to evaluate whether the product outputs capture characteristic global patterns and seasonality as well as impacts from known climate anomalies, including major droughts, occurring within the initial year of SMAP operations. These qualitative assessments were also used to determine whether there were any apparent model errors or anomalies requiring more detailed model and product error diagnostics. The L4_C model processing is conducted at a daily time step and 1-km spatial resolution consistent with MODIS fPAR and land cover (PFT) inputs. The L4_C product outputs are posted to a 9-km resolution global EASE-grid (version 2) consistent with the SMAP Level 4 daily soil moisture (L4_SM) inputs.  The primary daily product fields include vegetation gross primary production (GPP) and underlying environmental constraint (EC) metrics representing the proportion (%) of potential maximum rate levels defined for optimal (non-limiting) environmental conditions; EC reductions from potential conditions reflect unfavorable environmental effects, including high vapor pressure deficits, cold daily minimum air temperatures, low soil moisture levels and frozen soil conditions (Kimball et al. 2012). The L4_C product fields also include heterotrophic respiration (Rh) and underlying soil moisture (Wmult) and soil temperature (Tmult) EC metrics. The primary carbon variable used for L4_C validation assessment is net ecosystem $CO_2$ exchange (NEE), which is computed as a residual difference between GPP and ecosystem respiration defined as the sum of Rh and estimated autotrophic respiration.

Monthly averages of L4_C GPP daily outputs are presented in **Figure 7.1** for April, July, September, and December 2015.  These months represent respective spring green-up, peak growing season, fall onset, and peak senescence for Northern Hemisphere temperate, boreal and arctic ecosystems.  Also shown are the corresponding mean monthly EC constraint (Emult) metrics for estimated LUE and GPP.
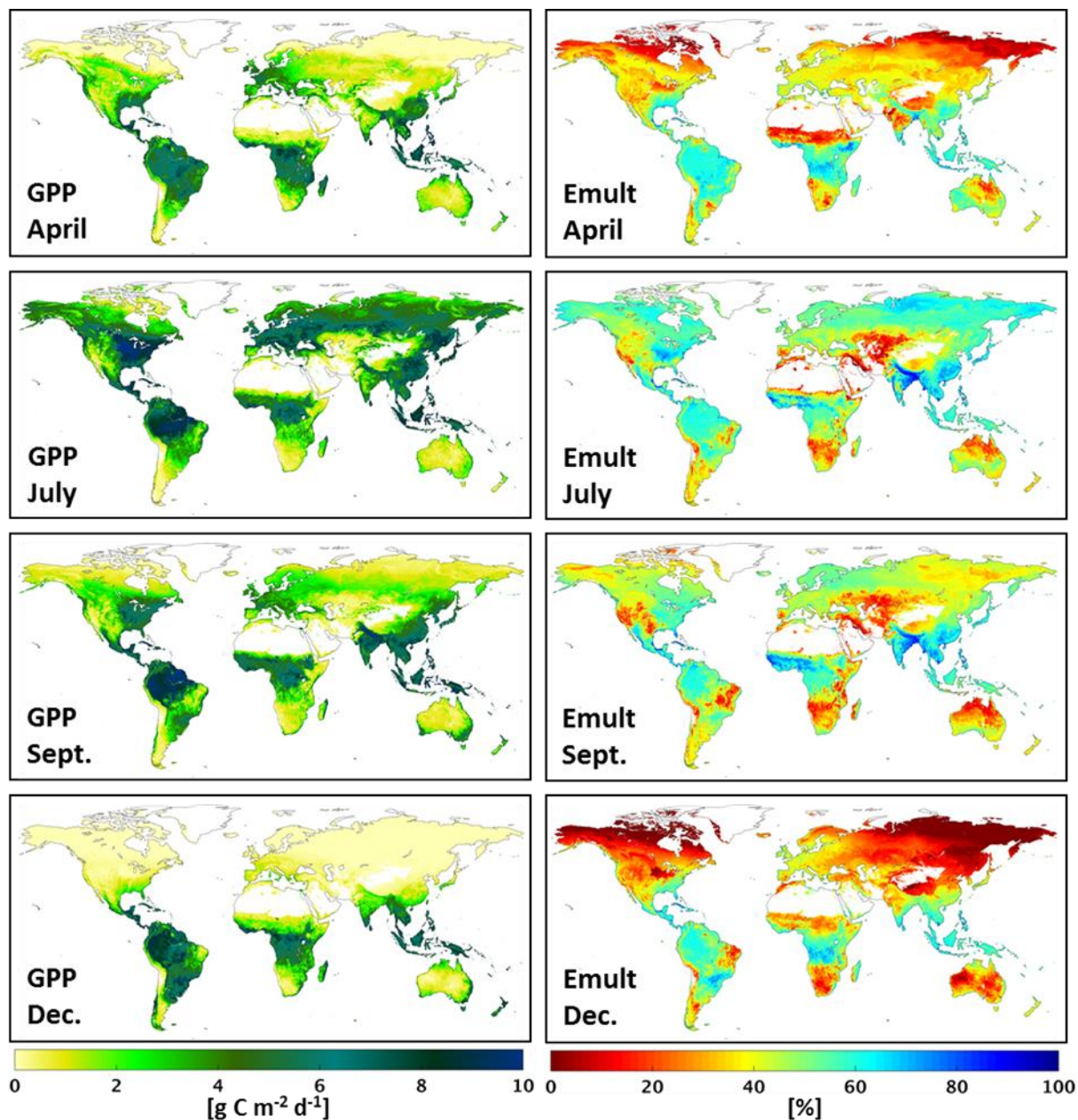
**Figure 7.1**. L4_C product monthly averages for April, July, September, and December 2015, showing vegetation gross primary production (GPP) and the GPP-based environmental constraint (Emult), which is the proportion (%) of estimated light use efficiency relative to a potential maximum rate ($LUE/LUE_{mx}$) defined for optimal (non-limiting) environmental conditions. The Emult metric is a dimensionless scalar ranging from 0 (fully constrained) to 100% (no constraint). White areas denote barren land, permanent ice, open water and other areas outside of the model domain.

These results depict the expected south-north progression of the Northern Hemisphere spring growing season onset and vegetation greening wave. Early spring conditions depicted by the April map show low productivity (GPP) over the northern latitudes from widespread cold temperatures and associated strong EC restrictions. In contrast, much higher productivity levels occur over the northern latitudes in July due to relatively warm, moist conditions and associated relaxation of EC constraints on LUE. July coincides with the peak of cropland productivity in the US Midwest region. Other regional anomalies are also

apparent in these images, including relatively low GPP levels and large EC restrictions over northern India resulting from a documented 2015 spring heat wave. Lower productivity areas are apparent over the southwest USA and African Sahel due to seasonal drought-induced soil moisture restrictions on estimated productivity. These results also show characteristic higher productivity over the tropics, indicating successful model screening and substitution of missing and cloud contaminated MODIS fPAR inputs using alternative clear-sky values from the ancillary MODIS 8-day fPAR climatology in the L4_C preprocessor.

**Figure 7.2** depicts the L4_C model-estimated soil heterotrophic respiration (RH) for the months of April, July, September, and December. The underlying cold temperature and low surface soil moisture EC constraints (Tmult and Wmult, respectively) to the RH calculation are also presented. These results show characteristically low respiration rates in early spring at higher latitudes prior to seasonal thawing, as indicated by strong Tmult reductions in the April image. In contrast, the Tmult constraints are relaxed after seasonal thawing with the arrival of warmer temperatures, resulting in widespread increases in Rh rates by July. However, the potential increase in RH is offset over many areas by surface soil moisture drying, including semi-arid areas of the southwest USA, central Asia, southern Africa, and central Australia.
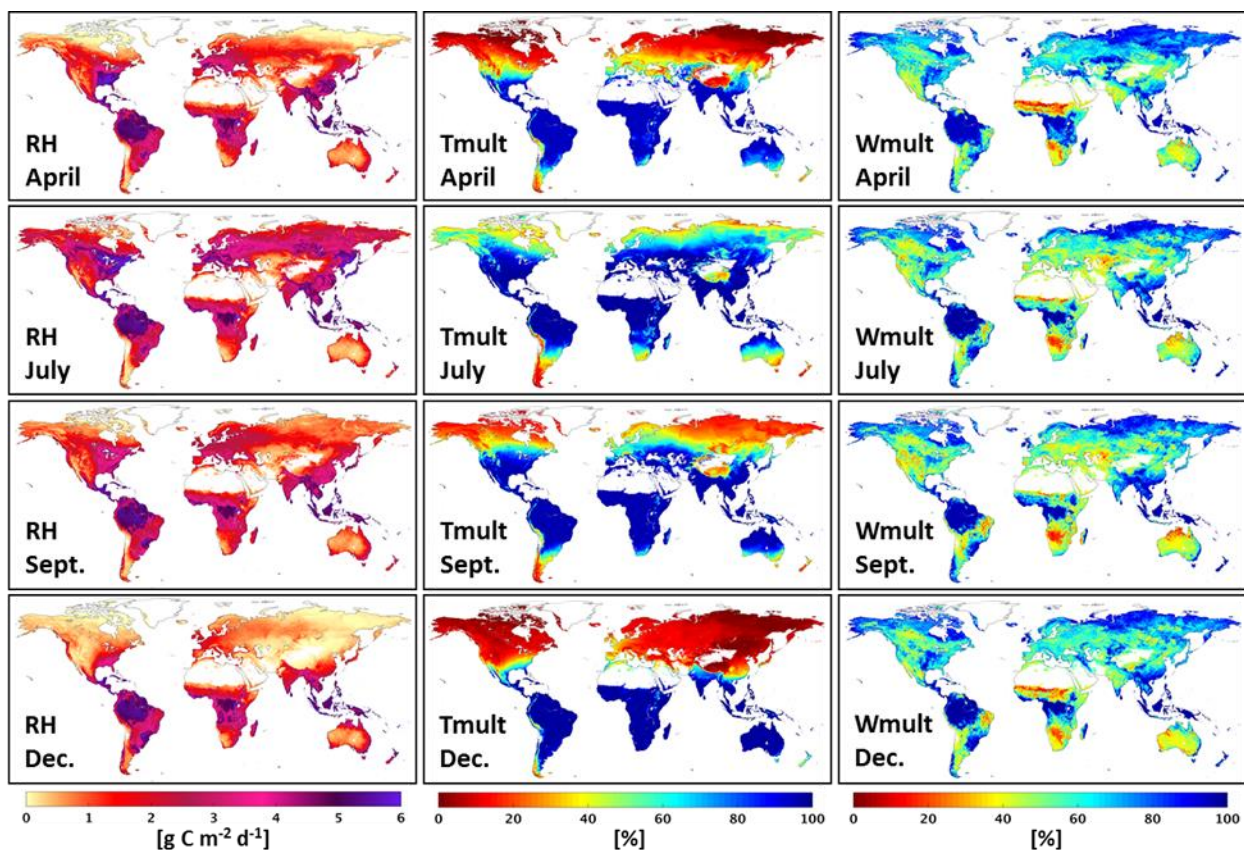


**Figure 7.2**. L4_C product monthly averages for April, July, September, and December 2015, showing heterotrophic soil respiration (RH) and RH-based environmental soil temperature (Tmult) and surface soil moisture (Wmult) constraint metrics, which is the proportion (%) of respired $CO_2$ relative to a potential maximum rate ($k_{opt}$) defined for optimal (non-limiting) environmental conditions. The Tmult and Wmult metrics are dimensionless scalars ranging from 0 (fully constrained) to 100% (no constraint). White areas denote barren land, permanent ice, open water and other areas outside of the model domain.

A selection of L4_C estimated daily NEE images extending from mid spring to early summer is presented in **Figure 7.3**. These maps show relatively large characteristic spatial heterogeneity in the sign and magnitude of the estimated carbon fluxes because NEE is a residual difference between much larger GPP and respiration fluxes. GPP and $R_{eco}$ also tend to respond similarly to environmental changes, which can obscure more obvious environmental impacts affecting carbon source/sink activity. Nevertheless, the sequence of images depicts the seasonal transition from early spring carbon source activity in the northern latitudes to widespread carbon sink activity with the arrival of warmer temperatures and vegetation greening in summer. Generally stronger carbon sink activity is also depicted over Eurasia relative to North America during the summer season due to anomalously warm, dry conditions reported over northwest Canada and Alaska in 2015. Likewise, the southwest USA and California show widespread and persistent carbon source activity stemming from an extended and severe drought in these areas.
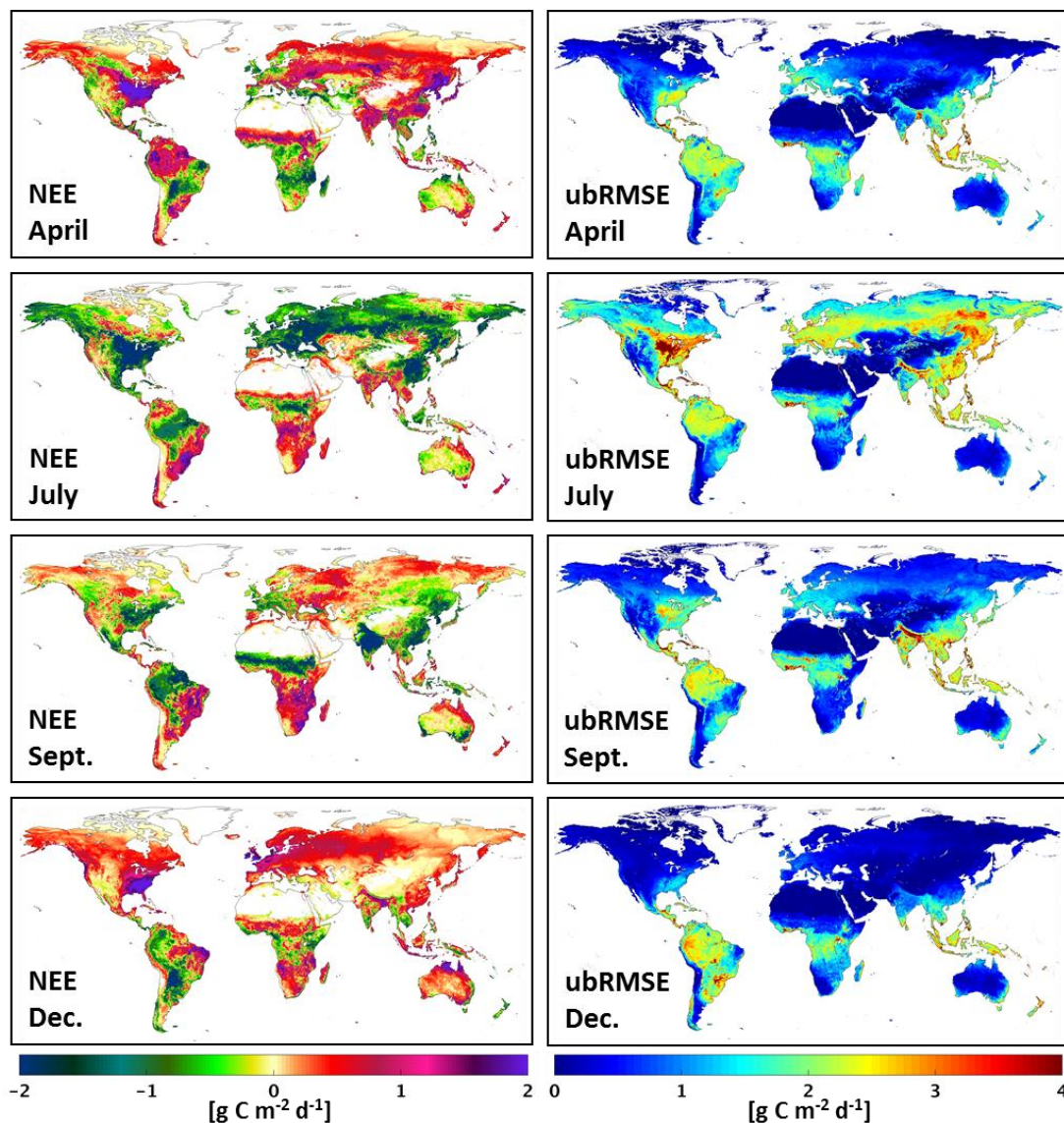


**Figure 7.3**. L4_C product monthly averages for April, July, September, and December 2015, showing Net Ecosystem $CO_2$ Exchange (NEE in units g C m$^{-2}$ d$^{-1}$) and associated L4C Quality Assessment (QA) ubRMSE (g C m$^{-2}$ d$^{-1}$). Negative NEE indicates net land $CO_2$ uptake from the atmosphere and positive indicates land $CO_2$ release to the atmosphere. White areas denote barren land, permanent ice, open water and other areas outside of the model domain.

The L4_C Quality Assessment (QA) parameter representing the estimated unbiased NEE RMSE (ubRMSE, g C m-2 d-1) is also shown in Figure 7.3. The ubRMSE parameter is generally proportional to the magnitude of the total estimated carbon flux (GPP+Reco) and is higher during peak seasonal productivity periods and in more productive PFT areas, including croplands and forests.

The L4_C surface soil organic carbon (SOC) field from the initial (April 2015) portion of the operational record is presented in **Figure 7.4**. The L4_C algorithms use a general three-pool soil decomposition model with cascading litter quality and associated soil decomposition rates encompassing variable turnover rates for labile, cellulosic and recalcitrant organic matter pools (Kimball et al. 2012, Yi et al. 2013). The SOC map in the figure represents the aggregation of these three soil carbon pools. These initial results largely represent carbon model spin-up conditions that reflect the daily climatological (2000-2013) forcing conditions from the GMAO SMAP Nature Run version 4 (NRv4) system used to initialize the L4_C model, including its SOC state at the beginning of the SMAP operational record. The observed SOC patterns generally capture the expected characteristic soil carbon distributions, including higher SOC stocks in cold northern boreal forest and tundra biomes estimated to hold more than half of the global soil carbon reservoir (Hugelius et al. 2014). The L4_C SOC map also shows relatively high soil carbon storage in temperate forest areas due to high forest productivity rates and cool, moist soils that promote soil carbon storage.  Low SOC areas occur over drier climate zones, including desert areas in the southwest USA with generally low productivity levels, warmer climate conditions and associated low SOC accumulations. The L4_C results also show relatively low SOC levels in tropical forests; high characteristic GPP rates and associated litterfall inputs are generally offset by warm, moist soil conditions that promote rapid decomposition in the soil, so that the majority of terrestrial carbon storage in the tropics is in vegetation biomass (Baccini et al. 2012).
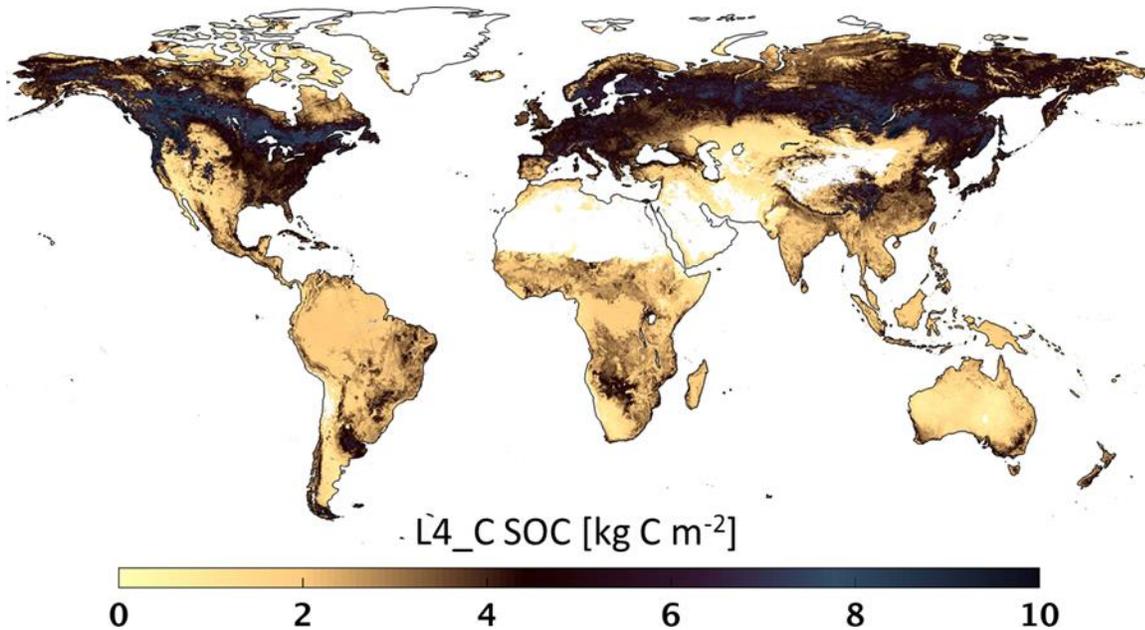


**Figure 7.4**.  Estimated surface (< 10 cm depth) soil organic carbon (SOC, kg C m-2) for April 15, 2015 from the SMAP L4_C operational record. The SOC estimates are derived at a 1-km spatial resolution during L4_C processing and posted to a 9-km resolution spatial grid. White areas denote barren land, permanent ice, open water and other areas outside of the model domain.

## 7.2  Global Performance against Historical Tower Observations

The L4_C validation assessment included comparisons of the model estimated daily carbon fluxes with ground-based observations of these variables from global sparse network tower eddy covariance $CO_2$ flux measurement sites as described in the SMAP Calibration/Validation Plan (Jackson et al. 2012). *In situ* data are critical in the assessment of the SMAP products. These comparisons provide for model performance and accuracy estimates and serve as a basis for modifying algorithms and/or parameters.  A robust analysis requires many sites representing a diverse range of vegetation and climate conditions. The L4_C assessment included comparisons of L4_C estimates of daily NEE and GPP against spatially collocated, gap-filled daily observations of these parameters from 228 tower sites spanning the global domain and representing the major global PFT classes. The tower records were obtained from a larger set of tower site records from the FLUXNET La Thuile tower data synthesis (Baldocchi 2008). The tower sites enlisted for the comparisons were selected on the basis of being located within relatively homogenous terrain and land cover (PFT) areas defined from MODIS 1-km land cover data within 9-km x 9-km windows centered over each tower site. The tower sites were also selected on the basis of having multi-year (2 or more years) observational records with relatively well characterized observation uncertainty.

The La Thuile tower record represents a global synthesis of FLUXNET daily tower observations where tower measurement records have been processed using consistent methods for temporal gap-filling of missing data, aggregation of daily carbon fluxes, and partitioning of NEE into component carbon fluxes.  However, the La Thuile data record only extended to 2007, so that comparisons with the L4_C product outputs were spatially co-located but were not temporally consistent. Therefore, these comparisons focused on evaluating L4_C-based NEE and GPP performance in relation to historical daily means and temporal variability (SD) at the 228 globally representative tower sites.

We conducted a spatial implementation of the L4_C error budget to map estimated ubRMSE performance for the NEE estimates over the global domain. Spatially explicit estimates of NEE ubRMSE (g C m$^{-2}$ yr$^{-1}$) were derived using a locally weighted forward model sensitivity analysis (Kimball et al. 2014) driven by MODIS fPAR and GMAO SMAP NRv4 daily surface meteorology inputs. The NRv4 data is derived using the same GEOS-5 land model underpinning the SMAP Level 4 Soil Moisture (L4_SM) product; these data were also used for calibration and initialization of the L4_C operational algorithms.  The resulting global NEE error budget is presented in **Figure 7.5**. The figure depicts the tower sites used for the model performance assessment and includes a summary plot showing the mean and range of variability in the correlations between the global tower NEE observations and associated L4_C NEE estimates stratified according to PFT class. The number of tower sites (N) represented within each PFT class is shown at the top of the plot, while NEE ubRMSE estimates are summarized for all land areas within each PFT class and in relation to the observed RMSE and ubRMSE differences and NEE correlations with the tower observations representing each PFT class.  These results indicate that approximately 66% and 83% of the global and northern (≥45°) domains are within the targeted L4_C product performance threshold for NEE (ubRMSE≤30 g C m$^{-2}$ yr$^{-1}$). The estimated ubRMSE global performance is largely consistent with local assessments derived from tower NEE observations representing the major PFT classes. The magnitude of the NEE RMSE differences are proportional to ecosystem productivity (GPP) so that more productive sites such as croplands have generally greater RMSE levels than less productive (e.g. shrubland and grassland) areas. Thus, if we express the NEE RMSE as a proportion of the overall flux magnitude (GPP + R$_{eco}$), which is always positive, the estimated extent of meaningful NEE estimates (i.e., ubRMSE/(GPP + R$_{eco}$) < 30%) increases to more than 80% of the global domain. Correlations between the model and tower NEE observations are generally greater in areas with larger characteristic seasonality, while EBF areas have lower correspondence largely due a smaller seasonal cycle in these predominantly tropical areas. Over northern land areas NEE ubRMSE levels are generally within the targeted accuracy threshold, except for some

northern croplands and forests. Overall, these results indicate that the L4_C algorithms and validated product are consistent with expected model design and performance specifications.
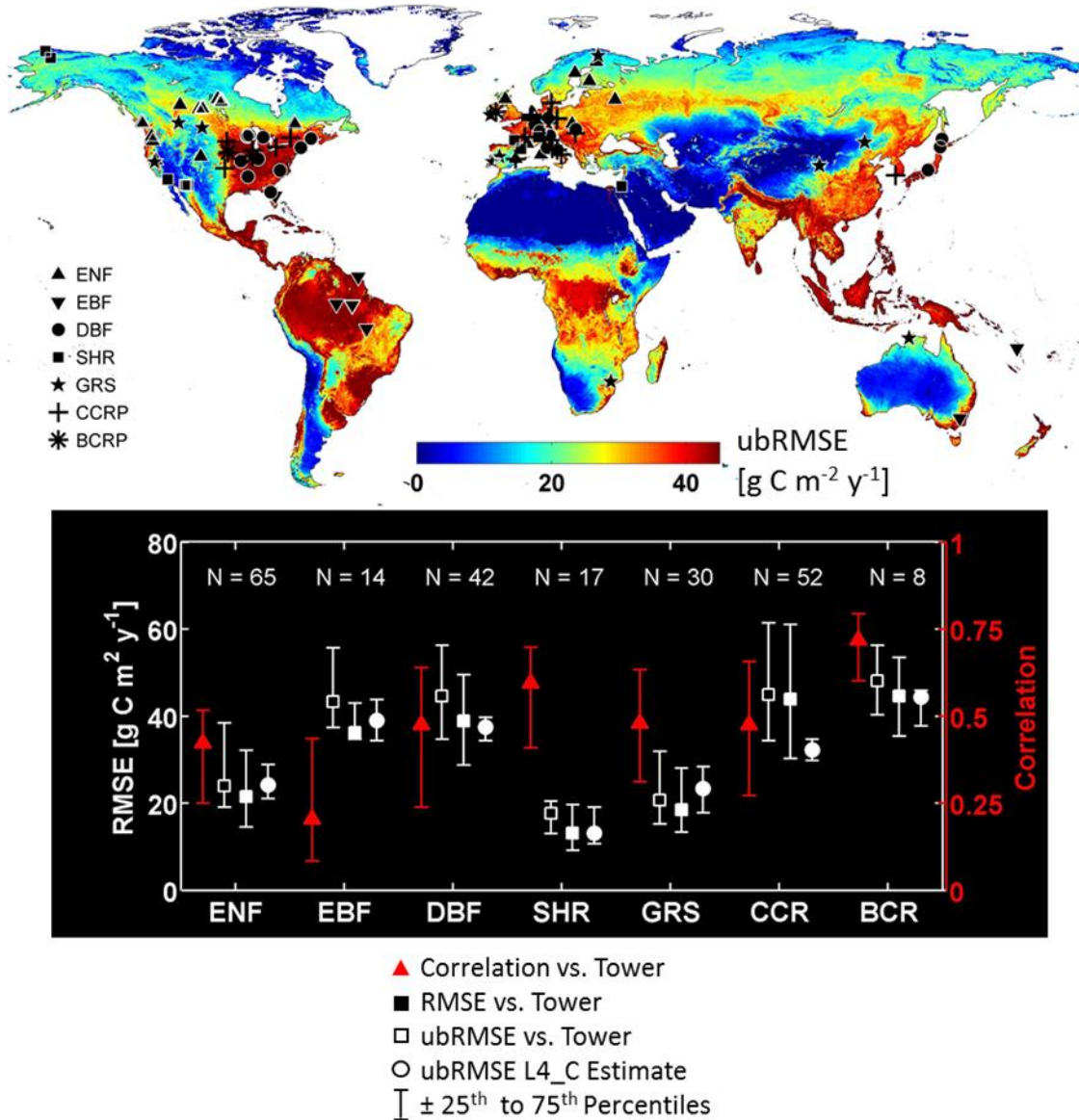


**Figure 7.5**. Estimated L4_C model and product performance for NEE in relation to in situ observations from 228 La Thuile tower sites representing the major global plant functional type (PFT) classes, including evergreen needleleaf forest (ENF), evergreen broadleaf forest (EBF), deciduous broadleaf forest (DBF), shrubland (SHR), grassland (GRS), cereal (C3) croplands (CCR) and broadleaf (C4) croplands (BCR). The tower sites are depicted in the L4_C model-estimated NEE ubRMSE (g C m$^{-2}$ yr$^{-1}$) map (top). The lower plot includes a summary of mean model and tower NEE correlations and RMSE differences within each PFT class, with associated 25$^{th}$ and 75$^{th}$ percentiles of spatial variability; the number (N) of La Thuile tower observation sites represented within each PFT class is denoted at the top of the plot. The estimated mean ubRMSE levels derived from the model sensitivity simulations (shown in upper map) for the tower pixel locations are also summarized within each PFT class in the plot.

We also compared L4_C outputs from the SMAP operational record against daily mean GPP and NEE values from the historical tower observations; here L4_C outputs within the initial year of SMAP

observations (Apr 2015 – Feb 2016) were compared against similar daily mean carbon fluxes from the 228 historical tower site records for the same seasonal period. The resulting spatial mean and variability (SD) in daily RMSE differences of the tower site comparisons within each PFT class are presented in **Figure 7.6**. Both total and unbiased RMSE values are presented. These results are similar to the global annual performance summary described above (**Fig. 7.5**), except that the performance assessment is conducted using the SMAP L4_C operational record. These results indicate that the L4_C performance for the validated release evaluation period is consistent with the algorithm design and targeted daily NEE accuracy threshold (ubRMSE$\leq$1.6 g C m$^{-2}$ d$^{-1}$) for relatively less productive PFT classes characteristic of northern biomes, whereas croplands and deciduous broadleaf forests show higher RMSE levels consistent with characteristic higher productivity levels and NEE rates for these vegetation types. Surprisingly, the L4_C model and tower RMSE values are low for relatively productive tropical forests (EBF); however, the seasonal variance of these ecosystems are characteristically low (leading to low ubRMSE) and the relatively few (14) towers representing this PFT class may not adequately represent global EBF diversity. The total RMSE levels are higher than the ubRMSE values due to systematic spatial and temporal bias in both model outputs and tower observations. The L4_C product performance is expected to improve with a longer SMAP observation record and continuing calibration refinements, and reprocessing updates to the lower order sensor retrievals and L4 product outputs.
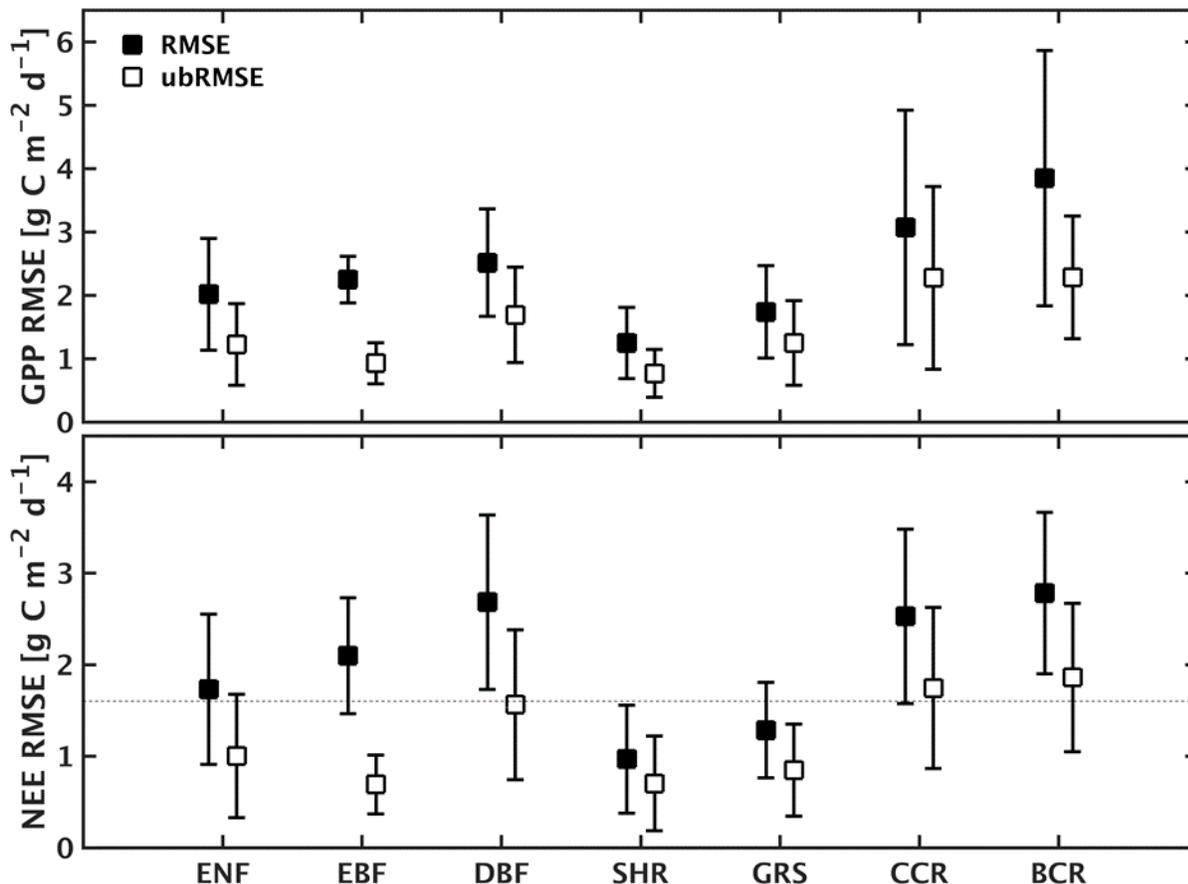


**Figure 7.6**. Spatial mean and variability (SD) in daily RMSE differences between L4_C operational outputs for GPP and NEE and daily mean C fluxes derived from historical daily tower observations at the 228 FLUXNET sites for the L4_C validated release evaluation period. The comparison results are summarized within global PFT classes representing individual tower sites. Both total (black squares) and unbiased RMSE values are presented. The targeted accuracy threshold for NEE (1.6 g C m$^{-2}$ d$^{-1}$) is also shown (dashed line).

## 7.3  Core Validation Sites

The L4_C operational daily outputs were compared against in situ daily tower observations for 26 participating core tower validation sites for the validated release evaluation period. Unlike the historical site comparisons described above, the CVS comparisons were both spatially consistent and temporally overlapping for the available 2015-2016 record. The CVS comparisons are enabled by active participation from individual tower site principle investigators (PIs) in the SMAP L4_C Cal/Val process. The SMAP L4_C CVS sparse tower network is summarized in **Table 7.1**; the associated tower CVS locations are presented in **Figure 7.7** along with the FLUXNET sites used for L4_C calibration and performance assessments (**Section 7.2**).

**Table 7.1**. CVS sparse tower network used for intensive L4_C product assessments. Shading indicates that adjacent sites share the same 9-km resolution L4_C grid cell for a total of 26 sites matched within 21 unique 9-km L4_C grid cells.

| Site[1] | PFT[2] | Lat. | Lon. | Location | Full Name |
|---|---|---|---|---|---|
| FI-Sod[3] | ENF | 67.36 | 26.64 | Finland | Sodankyla |
| CA-Oas | DNF | 53.63 | -106.20 | SK, Canada | SK-Old Aspen |
| US-ICt | SHR | 68.61 | -149.30 | AK, USA | Imnavait Creek Tussock |
| US-ICh | SHR | 68.61 | -149.30 | AK, USA | Imnavait Creek Heath |
| US-ICs | SHR | 68.61 | -149.31 | AK, USA | Imnavait Creek Sedge |
| US-PFa | DBF | 45.95 | -90.27 | WI, USA | Park Falls WLEF Tall Tower |
| US-BZs | ENF | 64.70 | -148.32 | AK, USA | Bonanza Creek Spruce |
| US-BZb | ENF | 64.70 | -148.32 | AK, USA | Bonanza Creek Bog |
| US-BZf | ENF | 64.70 | -148.31 | AK, USA | Bonanza Creek Fen |
| US-Atq | GRS | 70.47 | -157.40 | AK, USA | Atqasuk |
| US-Ivo | SHR | 68.47 | -155.73 | AK, USA | Ivotuk |
| US-SRM | SHR | 31.82 | -110.87 | AZ, USA | Santa Rita Mesquite |
| US-Wkg | GRS | 31.74 | -109.94 | AZ, USA | Walnut Gulch Kendall Grassland |
| US-Whs | SHR | 31.74 | -110.05 | AZ, USA | Walnut Gulch Lucky Hills |
| US-Ton | SHR | 38.43 | -120.97 | CA, USA | Tonzi Ranch |
| US-Var | SHR | 38.41 | -120.95 | CA, USA | Vaira Ranch |
| AU-Whr | SHR | -36.67 | 145.03 | Australia | Whroo |
| AU-Rig | CCR | -36.65 | 145.58 | Australia | Riggs Creek |
| AU-Ync | CCR | -34.99 | 146.29 | Australia | Yanco |
| AU-Stp | GRS | -17.15 | 133.35 | Australia | Sturt Plains |
| AU-Dry | GRS | -15.26 | 132.37 | Australia | Dry River |
| AU-DaS | GRS | -14.16 | 131.39 | Australia | Daly River Uncleared Savannah |
| AU-How | GRS | -12.50 | 131.15 | Australia | Howard Springs |
| AU-GWW[3] | SHR | -30.19 | 120.65 | Australia | Great Western Woodlands |
| AU-ASM | SHR | -22.28 | 133.25 | Australia | Alice Springs |
| AU-TTE | SHR | -22.29 | 133.64 | Australia | Ti Tree East |

[1]FLUXNET based tower site identifiers; [2]Tower PFT classes defined from a 1-km resolution MODIS (MOD12Q1) Type 5 global land cover map, consistent with L4_C processing. [3]Tower PI did not provide ecosystem respiration ($R_{eco}$) partitioned flux estimates.
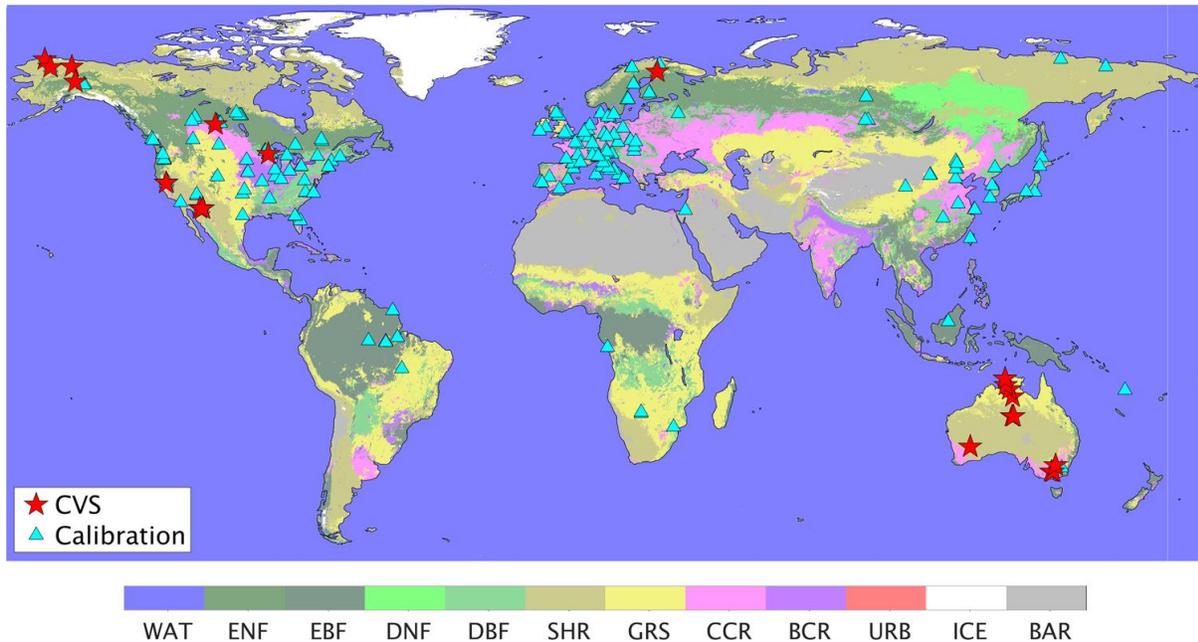
**Figure 7.7**. Locations of the core (CVS) tower validation sites used for intensive L4_C product assessments; FLUXNET sites with historical tower records used for the L4_C model calibration and performance assessments are also shown in relation to global plant functional types summarized from the MODIS MOD12Q1 (Type 5) global land cover classification.

Most of the CVS partners are providing near real-time daily tower observations, enabling temporally overlapping comparisons between the in situ tower observations and collocated SMAP L4_C operational product outputs. The CVS network spans 26 site locations and a broad range of climate and vegetation conditions; two of the sites (Imnavait, Bonanza Creek) include multiple towers sampling different vegetation communities within the larger sub-regions for a total of 26 participating CVS towers. Unlike the FLUXNET sites used for the L4_C global performance assessment (**Section 7.2**), the CVS towers may be located in spatially heterogeneous land cover areas with different PFT characteristics than the dominant vegetation class represented within the overlying 9-km resolution L4_C grid cell. Therefore, in addition to comparisons between tower observations and average daily model outputs for the corresponding overlying 9-km grid cell, the model-tower CVS assessment included comparisons between daily tower observations and mean L4_C product outputs from the most similar PFT class to the local tower footprint represented within the 9-km cell as determined from L4_C 1-km resolution processing and ancillary MODIS fPAR and land cover (MOD12Q1) inputs; the sub-grid PFT daily means derived from the 1-km resolution processing are preserved for each 9-km grid cell in the L4_C operational product outputs (Glassy et al. 2015).

Due to the CVS requirements for frequent (weekly) tower data delivery updates, uncertainty in the CVS tower records is expected to be larger than would otherwise occur from longer and more refined science data quality records. Local assessments of tower data quality were provided by many of the tower PIs as part of their data deliveries; the criteria and structure of the data quality metrics provided varied across the different tower sites, but they all give at least some qualitative indication of the reliability of the tower observations.

Comparisons of daily CVS tower carbon flux observations and corresponding L4_C product outputs are shown in **Figure 7.8** for selected representative northern tundra and temperate semi-arid shrubland sites spanning a large latitudinal climate gradient.  The underlying environmental constraint (EC) metrics

influencing the model GPP and $R_{eco}$ calculations are also shown. These results indicate that the L4_C product captures both daily and seasonal variability represented by the flux tower observations and corresponding with transient weather variability provided by SMAP L4_SM and other L4_C input datasets. The Ivotuk site indicates two notable NEE source (positive) anomalous daily events captured by the L4_C product during the month of July.  The first of these events correspond with seasonal peak soil temperatures, which promote increased $R_h$ (RH) in this moisture-abundant but cold temperature constrained tundra location.  The L4_C product also captures the NEE seasonal cycle at the Ivotuk site with the exception of higher-than-observed source activity during early spring and despite L4_C higher-than-observed GPP estimates.  The warmer Santa Rita shrubland site observations indicate that the L4_C NEE results match the characteristic seasonality of this strongly water-limited location, including two green seasons caused by early spring rainfall and a late summer monsoon.  These results illustrate the L4_C product ability to correctly represent NEE across diverse ecosystems spanning a wide range of characteristic climatic constraints.
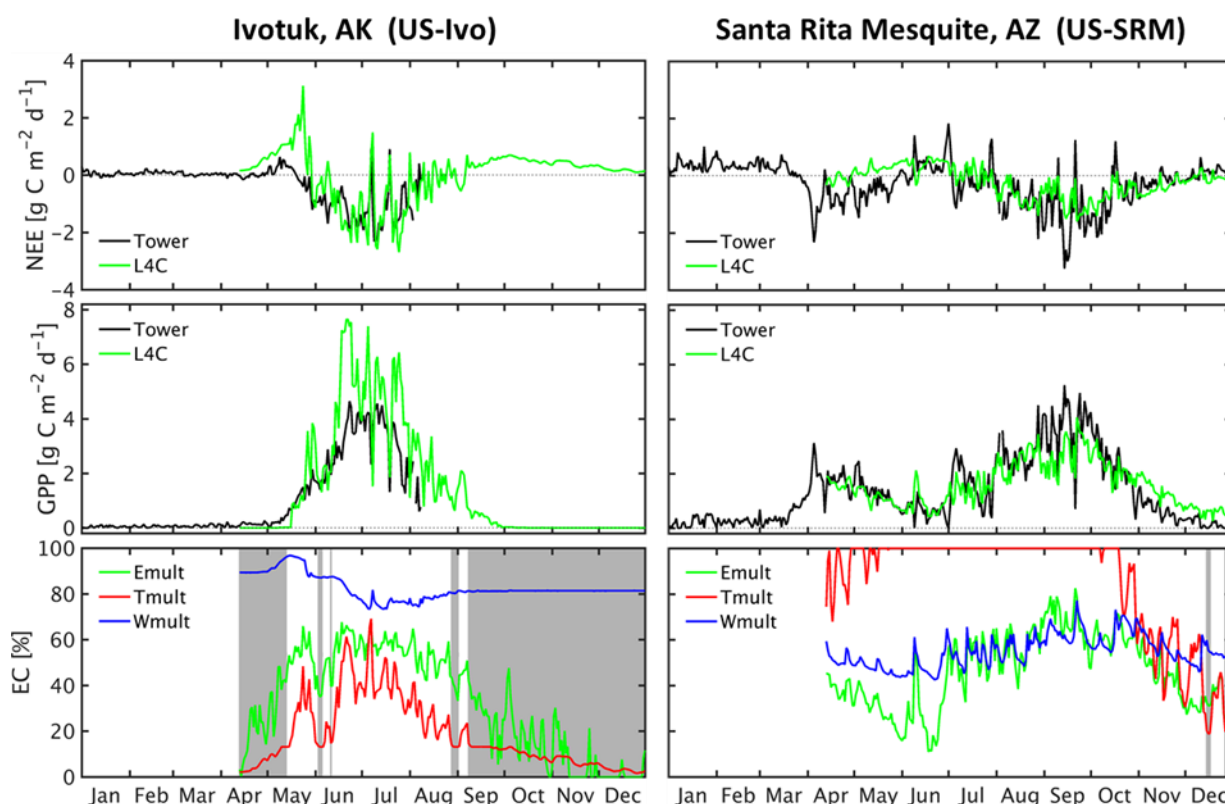


**Figure 7.8**.  L4_C time series (April 13, 2015 – December 31, 2015) examples for tussock tundra (Ivotuk) and semi-arid shrubland (Santa Rita Mesquite) CVS tower sites.  L4_C results shown for local tower PFT conditions (SHR for both locations with 85% and 17% of overlying 9-km L4_C grid cell coverage, respectively). Shaded regions indicate frozen conditions defined from the L4_C Frozen Area QA metric (Glassy et al. 2015).

The L4_C performance assessment against all available CVS daily tower observations for NEE, GPP and $R_{eco}$ is presented in **Figure 7.9**.  These results represent active CVS sites with tower records that have been quality checked and processed in a consistent format to facilitate the CVS analysis. These sites represent the CVS network listed in **Table 7.1**; remaining sites that were not evaluated for this submission had either non-overlapping data records or inconsistent formats at the time of this investigation. The reported metrics for each site include R, RMSE, and ubRMSE metrics computed between the tower observations and associated L4_C outputs representing daily mean carbon fluxes within the overlying 9-km resolution model grid cell; similar metrics are also derived for the model sub-grid PFT mean that is

most similar to the reported local tower footprint PFT. A detailed summary of the CVS comparison results aggregated according to representative PFT classes is presented in presented in **Table 7.2**.

**Table 7.2** Summary of L4_C and CVS tower comparison results for all locations (overall mean, shown in bold) and by tower PFT class. Counts (N) of individual locations includes redundant grid cells.  Partitioned $R_{eco}$ not reported for FI-Sod (ENF) and AU-GWW (SHR) tower sites; these locations were therefore included for NEE and GPP summary statistics but not $R_{eco}$ leading to differing counts (N) of individual sites represented for the ENF and SHR PFT classes.

| | NEE [g C m$^{-2}$ d$^{-1}$] | | | | GPP [g C m$^{-2}$ d$^{-1}$] | | | | $R_{eco}$  [g C m$^{-2}$ d$^{-1}$] | | | |
|---|---|---|---|---|---|---|---|---|---|---|---|---|
| | R | RMSE | ubRMSE | N | R | RMSE | ubRMSE | N | R | RMSE | ubRMSE | N |
| **Overall** | **0.52** | **1.04** | **0.79** | **26** | **0.72** | **1.27** | **0.85** | **26** | **0.65** | **1.16** | **0.62** | **24** |
| **ENF** | 0.57 | 1.07 | 0.90 | 4 | 0.85 | 1.35 | 1.16 | 4 | 0.72 | 1.44 | 1.23 | 3 |
| **DNF** | 0.67 | 2.27 | 2.07 | 1 | 0.90 | 3.08 | 2.04 | 1 | 0.80 | 1.63 | 1.44 | 1 |
| **DBF** | 0.58 | 3.40 | 2.15 | 1 | 0.85 | 2.05 | 2.02 | 1 | 0.88 | 3.34 | 0.74 | 1 |
| **SHR** | 0.53 | 0.78 | 0.63 | 12 | 0.64 | 1.04 | 0.61 | 12 | 0.63 | 0.96 | 0.45 | 11 |
| **GRS** | 0.33 | 0.95 | 0.62 | 6 | 0.73 | 1.12 | 0.64 | 6 | 0.65 | 0.81 | 0.48 | 6 |
| **CCR** | 0.88 | 0.98 | 0.72 | 2 | 0.82 | 1.59 | 1.10 | 2 | 0.51 | 1.55 | 0.54 | 2 |

Overall, the CVS comparisons indicate favorable L4_C product accuracy in relation to independent tower measurement based daily carbon flux observations (**Fig. 7.9**). The L4_C based NEE results are generally within the targeted accuracy threshold (ubRMSE $\leq$ 1.6 g C m$^{-2}$ d$^{-1}$) relative to the CVS observations for northern ($\geq$45°N) boreal forest and tundra tower sites, with generally favorable correspondence across all sites for NEE, GPP and $R_{eco}$ (R=0.52, 0.72, and 0.65, respectively, with p<0.005). The L4_C results are also favorable for semi-arid grassland, shrubland, and cropland tower sites, which show large seasonal variations in carbon fluxes and underlying soil moisture conditions.  The R correspondence was generally lower for sites with a smaller seasonal cycle, coinciding with lower ubRMSE. L4_C was unable to correctly represent GPP seasonality (R=-0.26) for site AU-ASM because eucalyptus trees locally access groundwater in this otherwise arid location (PI personal communication). The ubRMSE levels between the CVS observations and L4_C carbon fluxes were larger for relatively productive temperate deciduous forest sites, including Park Falls (US-PFa). The relative L4_C product accuracy was lower where PFT representation between the local tower footprint and overlying product grid cell was less consistent, including Old Aspen (CA-Oas) and Howard Springs (AU-How) sites. Product accuracy was generally improved by comparing the tower observations to the closest matching L4_C model PFT class represented within the overlying 9-km grid cell. However, for the CA-Oas and AU-How sites, the MODIS 1-km resolution global land cover classification does not adequately characterize the local land cover represented within the tower footprint.  CA-Oas is a broadleaf deciduous aspen stand surrounded by dominant evergreen needleleaf forest, whereas AU-How is a eucalyptus savannah which MODIS classifies as grassland.  In such cases, GPP from the tower observations is significantly higher than represented by L4_C product outputs, although the L4_C product still generally captures GPP seasonal and daily variability.

The L4_C product NEE ubRMSE Quality Assessment (QA) parameter corresponds well with the observed NEE RMSE and ubRMSE levels computed from the tower observations across all CVS sites (**Fig. 7.10**).  As expected, the QA correspondence is lower for RMSE relative to ubRMSE ($R^2$ = 0.52 vs $R^2$ = 0.59, respectively; p<0.05) because the L4_C ubRMSE QA metric considers only random errors in L4_C model input fields.  Since NEE errors tend to scale with flux magnitude (GPP + $R_{eco}$), flux magnitude automatically provides error predictive power. Nevertheless, the observed strong correspondence between L4_C and CVS observations indicates that the product correctly reproduces the correspondence of higher error with greater carbon flux magnitude; much of L4_C random error is also explained by uncertainty in the model input datasets.  Additional random and systematic errors not

captured by the L4_C RMSE QA metric include model misrepresentation or parameterization of key processes; sub-grid scale heterogeneity and land cover mismatches between model processes and the local tower footprint; and local ecological factors not explicitly represented in the L4_C model assumptions and calculations, including the modification of carbon stocks from disturbance (e.g. wildfire), abiotic litter and SOC decomposition/volatilization, land management (e.g. irrigation, fertilization, crop rotation) and land cover and land use changes.
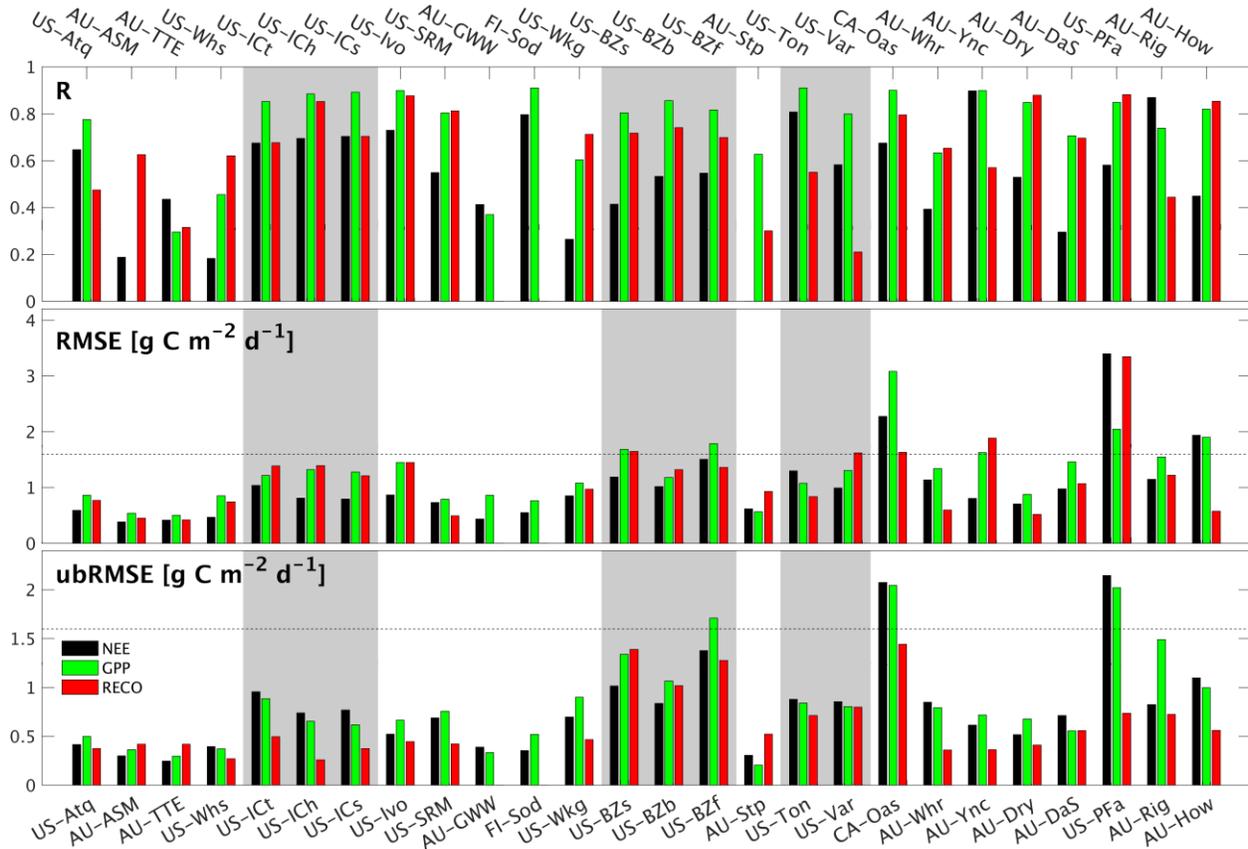


**Figure 7.9**. Summary of CVS comparisons between daily tower observations and L4_C daily product outputs for GPP and NEE within the initial operational record. Sites are sorted from left to right in order of increasing annual flux magnitude (GPP + $R_{eco}$). The reported metrics include R correspondence, RMSE and ubRMSE. The targeted daily NEE RMSE threshold for the L4_C product (1.6 g C m$^{-2}$ d$^{-1}$) is shown as a dashed line. Gray shading denotes CVS towers within the same overlying 9-km L4_C grid cell. Tower PIs for sites FI-Sod and AU-GWW did not report $R_{eco}$, therefore associated statistics were omitted. GPP correlation negative (R=-0.26) for AU-ASM.
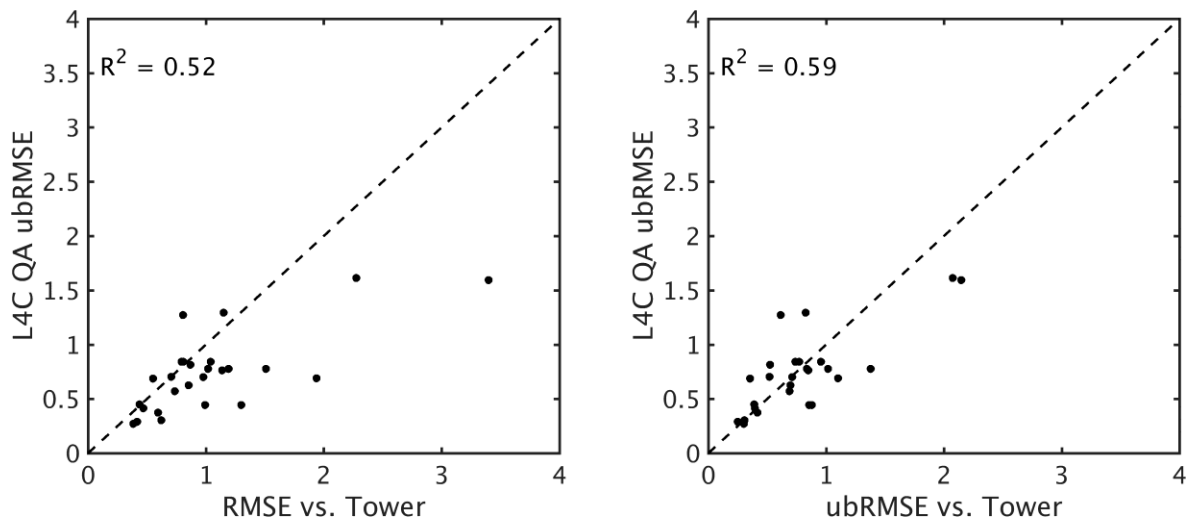
**Figure 7.10**. Comparison of NEE mean daily ubRMSE (g C m$^{-2}$ d$^{-1}$) estimated by the L4_C NEE Quality Assessment (QA) parameter vs. NEE RMSE (left) and ubRMSE (right; g C m$^{-2}$ d$^{-1}$) computed between daily L4_C and tower observations for the 26 CVS locations. Dashed line represents 1:1 correspondence. The L4_C daily ubRMSE QA estimates are aggregated to quadratic means for the initial assessment period for comparing L4_C vs. tower RMSE statistics at each tower site.

The CVS comparisons reveal several challenges associated with maintaining robust quality control over a diverse set of tower observations and participating Cal/Val partner teams, despite efforts to standardize data formatting and submission of frequent tower observation updates. The CVS tower observations have larger uncertainty relative to longer historical data records such as the La Thuile FLUXNET record (Section 7.2). The larger tower observation uncertainty is due to multiple factors, including project requirements for frequent updating of tower data, which restricts the amount of time available for detailed post-processing analysis and data quality checks. The relatively short (<1-yr) period of record for the CVS observations also contributes to larger uncertainty associated with gap-filling of missing data and estimation of component carbon fluxes (e.g. GPP, $R_{eco}$) from the tower NEE measurements. Additional uncertainty of component fluxes (e.g. GPP, $R_{eco}$) arise from inconsistencies in methods of flux partitioning used by individual PIs which may not be well-documented. These factors lend somewhat reduced confidence to component carbon flux estimates relative to NEE, although processing details (ustar corrections, etc.) of NEE also vary among individual PIs. While many of the CVS partners contributed data quality metrics, these data generally represented simple quality flags and other qualitative indicators, while underlying methods and criteria used to define these metrics also varied by tower location.

# 7.4 Consistency with Other Global Carbon Products

The L4_C product outputs were compared against similar variables from other available global carbon products. The objective of these comparisons was to assess and document the general consistency of selected L4_C operational product fields in relation to similar variables from other global benchmark datasets commonly used by the community. The global data products examined are publicly available and include:

1) The NASA EOS MODIS MOD17A2 (C5) operational GPP product, with 1-km resolution and 8-day temporal fidelity (Zhao and Running, 2010);

2)   The Max Planck Institute's Model Tree Ensemble (MPI-MTE) based global tower observation upscaling of monthly GPP from the La Thuile FLUXNET synthesis observational record (Jung et al. 2011);

3)   Solar-Induced canopy Fluorescence (SIF) satellite observations from the ESA GOME-2 (Global Ozone Mapping Experiment) and NASA Orbiting Carbon Observatory (OCO-2) sensors, which were used as a proxy for GPP (Joiner et al. 2013, Frankenberg et al. 2014);

4)   Global carbon model inversion based estimates of biological $CO_2$ surface exchange (NEE) from NOAA ESRL CarbonTracker as represented by regionally optimized GFED-CASA priors (Peters et al. 2007);

5)   Global soil organic carbon (SOC) inventory records from the International Geosphere Biosphere Program Data Information System (IGBP-DIS; Global Soil Data Task Group 2000) and the Northern Circumpolar Soil Carbon Database (NCSDC; Hugelius et al. 2014).

Global consistency checks between the L4_C GPP outputs and benchmark productivity datasets involved comparing mean latitudinal distributions of average product fields for the initial evaluation period (Apr 2015 – Feb 2016) against average conditions for the same seasonal period derived from the other data records. The MODIS MOD17A2 and MPI-MTE GPP records used for this analysis extended from 2000 to 2014 and from 2000 to 2011, respectively. The GOME-2 SIF record (version 26) used for this study represented composited mean monthly observations extending from 2007-2015, while the NASA OCO-2 SIF observations (LITE Files version B7000) extended from 2014-2015. The SIF retrievals from GOME-2 and OCO-2 are related to LUE and photosynthesis and were used as an observational proxy for GPP.

The biological $CO_2$ surface exchange estimates from CarbonTracker (version CT2013B) are derived from GFED-CASA land model estimated priors, optimized by regional scaling factors estimated using EnKF atmospheric transport model (TM5) inversions ingesting ship and flask atmospheric $CO_2$ concentration measurements. CarbonTracker CT2013B biological fluxes are provided in monthly timesteps on a $1° \times 1°$ global grid for the period 2000-2013. Unfortunately the CT data do not currently overlap with the L4_C operational period, but allow for comparison against the L4_C estimated seasonal climatology determined from SMAP NRv4 inputs (covering 2001-2013); together these comparisons provide historical context for evaluating the L4_C operational results. The L4_C NEE climatology results were also rescaled to match the CT estimated carbon flux means and standard deviations. This rescaling is justified because L4_C model is initialized to steady-state SOC conditions and the carbon source/sink magnitude of CT is regionally determined by the CT EnKF data assimilation system. Presumably the L4_C carbon source/sink magnitude would likewise be rescaled if it were to replace GFED-CASA land model priors in a similar inversion system. The SMAP L4_C NEE results were compared against the CT based $CO_2$ surface exchange estimates derived from observed changes in global atmospheric $CO_2$ concentrations, while accounting for estimated $CO_2$ contributions from fire, ocean and anthropogenic activity. The CT and L4_C results were then aggregated to a monthly time step and mean latitudinal gradient and compared over the SMAP observation record.

The available SOC inventory records represent static maps extending over global (IGBP-DIS) and northern (NCSCD) domains. Surface (<10cm depth) SOC stocks were estimated as a fixed proportion (33.33%) of the total soil profile (0-100 cm depth) SOC stock records. These data were compared against the initial L4_C SOC product outputs from April, 2015. The SOC records were evaluated by comparing latitudinal means and spatial SD ranges. A global SOC difference map was also computed between the L4_C and IGBP-DIS records to evaluate the spatial pattern of SOC differences. Detailed summaries of these comparisons are provided in the following sub-sections.

## *7.4.1  GPP Assessment against Other Global Benchmarks*

The L4_C daily GPP product fields were averaged over the operational evaluation period and compared against other observational benchmark global vegetation productivity datasets, including the NASA MODIS MOD17 (Zhao and Running, 2010) and MPI-MTE (Jung et al. 2011) GPP products.  The long-term (2000-2014) MOD17 GPP record is available with 8-day temporal repeat and was aggregated to produce a climatological mean daily record for the same (Apr-Feb) evaluation period. The averaged MODIS GPP data was then re-projected from a 5-km resolution geographic projection to the 9-km resolution global EASE-grid (V.2) format of the L4_C product using nearest-neighbor resampling.  The MPI-MTE GPP record is available at a monthly time step and extends from 2000-2011 (Jung et al. 2011). The MPI record is derived using a Model Tree Ensemble (MTE)-based machine learning algorithm and empirical upscaling of tower-based daily GPP observations from the global FLUXNET data archive. The MTE spatial upscaling approach also uses 29 explanatory geospatial variables, including monthly fPAR from the SeaWiFS satellite sensor. The monthly MPI GPP data were re-projected from a 0.5 degree spatial resolution and geographic projection to the 9-km resolution global EASE-grid (V.2) format using nearest-neighbor resampling, and then aggregated to produce a climatological mean daily record for the Apr-Feb seasonal evaluation period.

The satellite based GPP records for the Apr-Feb period were also evaluated against satellite Solar-Induced canopy Fluorescence (SIF) retrievals, where SIF was used as a more direct observational proxy for GPP.  The SIF observations were obtained from two sources, including the ESA GOME-2 record (V.26) extending from 2007-2015 (Joiner et al. 2013), and the NASA OCO-2 record (V.B7000) extending from 2014-2015 (Frankenberg et al. 2014). The GOME-2 SIF (740nm) data are available as composited monthly means with 0.5 degree spatial resolution and geographic projection format. The OCO-2 SIF (757nm) data were obtained as daily files geolocated (WGS84) to the center of the sensor footprint. The OCO-2 data represent nadir-view converged soundings that passed initial quality criteria thresholds and included a daily SIF correction for non-fluorescing surfaces. Both the GOME-2 and OCO-2 SIF data were aggregated to the same Apr-Feb climatology and EASE-grid format for comparison with the other GPP products.  The global GPP and GOME-2 SIF patterns were compared, while the spatial means of the GPP and SIF products were computed along 0.05 degree latitudinal bins; the correspondence (R) and significance of the mean latitudinal distributions were also evaluated in relation to the OCO-2 SIF record.

The global comparison of mean daily GPP and SIF records are presented in **Figure 7.11**. The L4_C GPP record shows a generally consistent global productivity pattern relative to the MOD17 and MPI-MTE GPP benchmarks. The L4_C GPP results also show a similar global productivity pattern in relation to the SIF observations from GOME-2. While SIF is proportional to canopy absorbed photosynthetically active radiation (APAR) and photosynthesis, the relationship between SIF (mW m$^{-2}$ sr$^{-1}$ nm$^{-1}$) and GPP (g C m$^{-2}$ d$^{-1}$) can vary according to vegetation type and environmental conditions (Porcar-Castell et al. 2014); however, the relative global patterns of SIF and GPP are expected to be largely consistent. The SIF and GPP records all show similar global productivity distributions, including higher productivity rates in the tropical and temperate zones, and lower productivity levels at higher latitudes and drier climate zones. However, the L4_C results show generally higher mean latitudinal correspondence with the OCO-2 SIF benchmark (R = 0.87) than the other GPP products (0.75≤ R ≤0.81). The L4_C GPP correlation is also similar to the relationship between GOME-2 and OCO-2 SIF records (R = 0.88). There are also notable differences between the GPP and SIF products. The SIF data indicate generally higher productivity rates over croplands, which may be due to incorrect model parameterization and underestimation of optimal light use efficiency levels for intensively managed cropland vegetation (Guanter et al. 2013, Madani et al. 2014); however, the MOD17 and MPI-MTE GPP results indicate generally larger underestimation of cropland productivity levels than the L4_C results.  Other differences in the productivity patterns are partially attributed to the coarser spatial footprint and temporal compositing of the SIF observations relative to the finer (1-9 km) resolution of the L4_C processing, and climate variability between the L4_C

sampling period (Apr, 2015 – Feb, 2016) and average conditions defined from the longer GPP and SIF records.
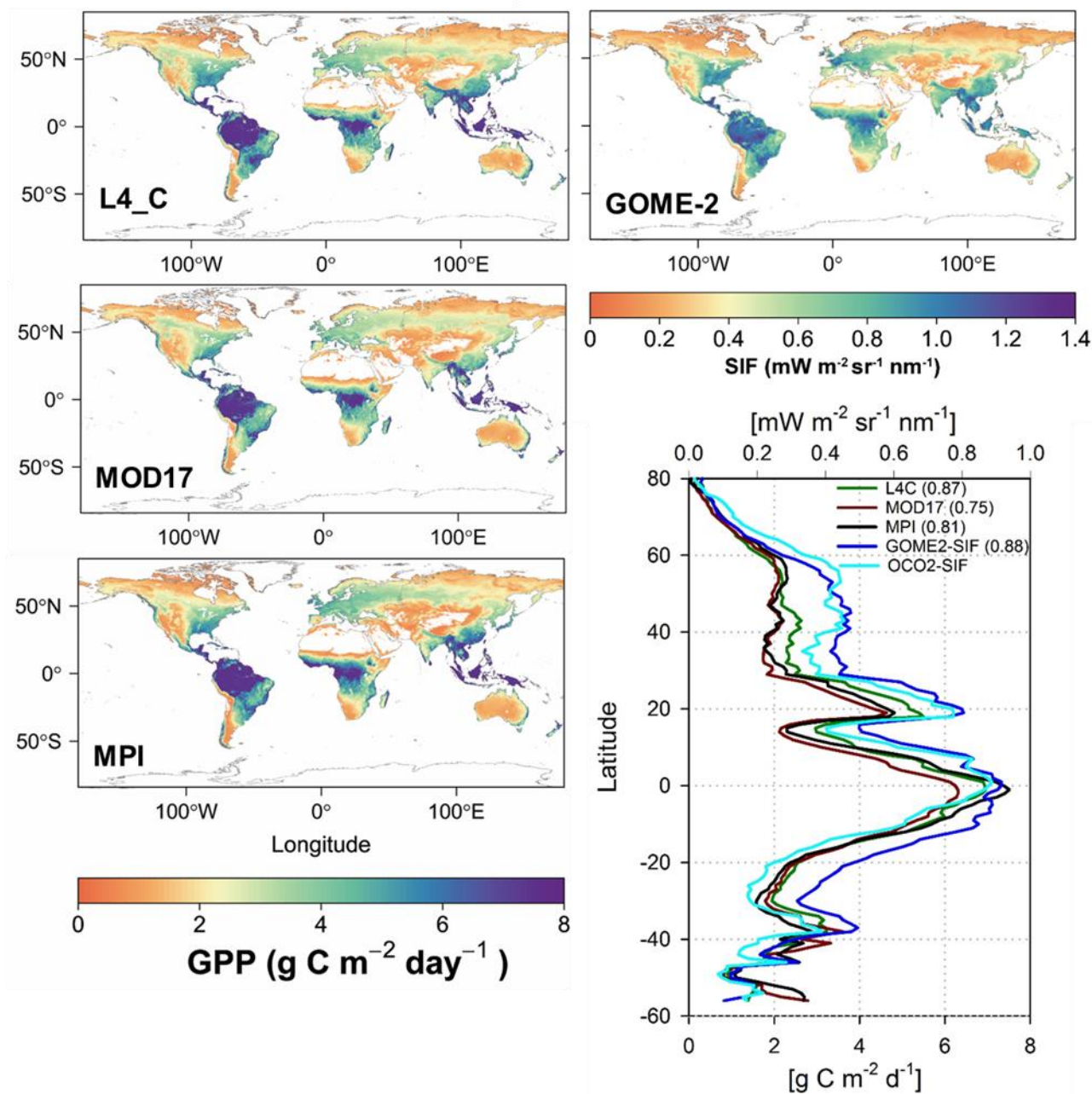


**Figure 7.11**. Comparison of mean daily GPP outputs (g C m$^{-2}$ d$^{-1}$) from the SMAP L4_C product in relation to other productivity benchmarks, including GPP from MOD17 and MPI-BGC, and SIF (mW m$^{-2}$ sr$^{-1}$ nm$^{-1}$) from GOME-2 and OCO-2. Here SIF is used as a proxy for GPP even though the relationship between GPP and SIF can vary, particularly under environmental stress. The L4_C outputs are derived from the initial (Apr, 2015 - Feb, 2016) data record, and compared against mean GPP and SIF values for the same climatological period derived from the other multi-year observational data records. The global GPP patterns (left) are shown in relation to GOME-2 SIF (top right). The latitudinal mean GPP and SIF distributions are also shown (lower right), including correlations (in parentheses) between these parameters and the OCO-2 baseline. White areas in the maps represent barren land, permanent ice, open water bodies and other areas outside of the L4_C product domain.

## *7.4.2  NEE Assessment using CarbonTracker*

The SMAP L4_C NEE results were compared against the CarbonTracker (CT2013B) based $CO_2$ surface exchange estimates derived from observed changes in global atmospheric $CO_2$ concentrations, while accounting for estimated $CO_2$ contributions from fire, ocean and anthropogenic activity. The CT and L4_C results were then aggregated to a monthly time step and mean latitudinal gradient and compared over the SMAP NRv4 defined annual climatology and for the L4_C operational record.

The L4_C results compare favorably with the overall CT seasonal and spatial patterns, but with some notable differences (**Fig. 7.12**).  Whereas the L4_C and CT results show similar spatial patterns for the tropics and US croplands for the month of July, the L4_C NEE outputs show more widespread carbon sink activity in Northwestern North America than CT, but much weaker sink activity across Siberia, Northern Eurasia, and boreal forests of central Canada. The central Canadian boreal forests were anomalously dry in 2015, which the L4_C results seem to capture in the form of reduced carbon sink strength relative to the L4_C and CT climatological outputs.  This pattern is also evident in the >60ºN latitudinal band, for which the L4_C results show ≈26% reduction in peak carbon uptake during 2015. The L4_C seasonal uptake cycle leads the CT cycle by approximately two weeks for the 30ºN-60ºN band and yet lags the spring zero-crossing for the 0ºN-30ºN band by the same amount, whereas the fall zero-crossing for the 0ºN-30ºN band remains in-phase.  For the Southern Hemisphere, L4_C and CT seasonality closely match with the exception of increased CT uptake during August for the 0ºS-30ºS band.  Interestingly, this feature is caused by a much stronger carbon sink in the southeastern Amazon than suggested by the L4_C results (not shown). These patterns indicate potential for the L4_C product to inform atmospheric inversion studies, although further investigation is required to more fully understand these differences and their underlying environmental controls.
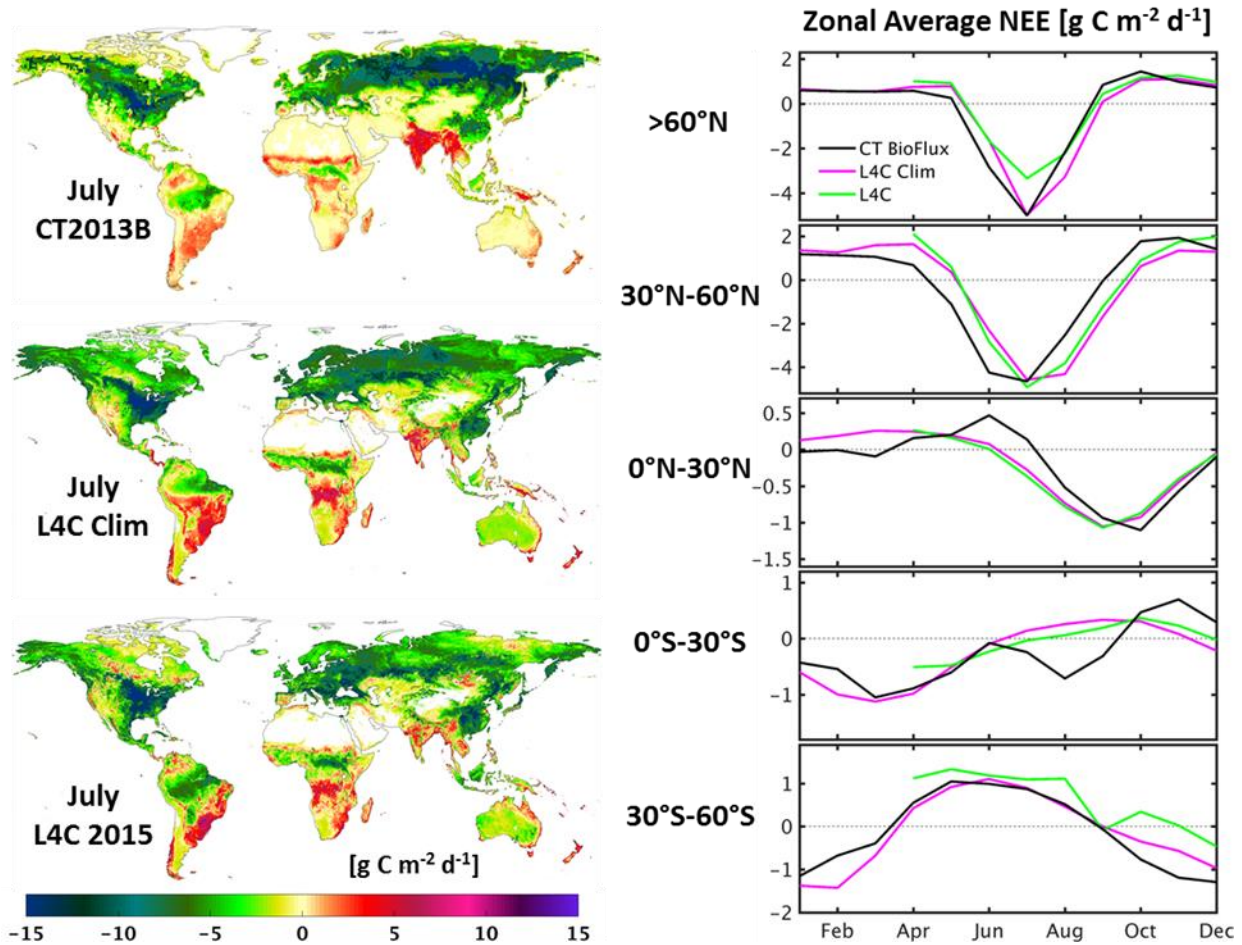
**Figure 7.12**. Comparison of mean monthly NEE (g C m$^{-2}$ d$^{-1}$) from the SMAP L4_C product in relation to monthly mean biological $CO_2$ surface exchange estimates from CarbonTracker (2000-2013) partitioned by latitudinal zones (right). The L4_C results are given for the mean monthly climatology (2000-2013) and operational record (April 13-Dec 31, 2015).  Global maps of NEE carbon source/sink patterns for July are shown (left). CT and L4_C maps are shown in their native resolutions, 1°×1° and 9-km, respectively.  SMAP L4_C climatology and 2015 mean and standard deviations are rescaled to match CT mean and standard deviations.

## 7.4.3  Soil Carbon Assessment against Global Inventory Records

The L4_C SOC stock estimates from the initial April 2015 record were compared against available static SOC inventory records extending over global (IGBP-DIS) and northern (NCSCD) domains. The L4_C SOC fields are computed on a daily basis as the residual difference between estimated litterfall inputs from vegetation net primary production, and soil heterotrophic respiration losses from the decomposition of soil organic matter. The L4_C SOC estimates are approximately representative of upper soil (<10 cm depth) conditions determined from the surface soil moisture (Wmult) and temperature (Tmult) constraints to the R$_h$ calculations (Kimball et al. 2012).  Therefore, surface SOC stocks were estimated from the IGBP and NCSCD global inventory data as a fixed proportion (33.33%) of the reported total soil profile (0-100 cm depth) SOC stock records, though the actual proportion can vary from approximately 29 to 57 percent or more (Jobbagy et al. 2000). These data were then compared against the initial L4_C SOC product outputs from April, 2015. The IGBP and NCSCD maps were re-projected from a 0.5 degree spatial resolution and geographic projection to the 9-km resolution global EASE-grid (V.2) format of the L4_C product using nearest-neighbor resampling.  A global SOC difference map was then computed by

grid cell-wise subtraction of the estimated IGBP surface SOC values from collocated L4_C SOC values. The distributions of the SOC spatial means and ±1 SD spatial variations were also computed along 0.05 degree latitudinal bins and compared for relative consistency between the inventory records and L4_C data. The NCSCD record is only available for the northern land areas, while the IGBP record extends over the global domain.

The resulting L4_C and IGBP global SOC difference map and the mean latitudinal distributions of the different SOC estimates are presented in **Figure 7.13**. The latitudinal SOC distribution indicated by the L4_C record is similar to the soil inventory records, though the L4_C results are generally at the lower range of the reported inventory data. The L4_C results show a similar increase in SOC levels at higher latitudes consistent with characteristic soil carbon storage increases in colder boreal and tundra soils. The difference map between the L4_C and IGBP results indicates larger model underestimation in northern boreal forest and tundra areas known to contain a large portion of the global soil carbon stock stored in permafrost soils, which have accumulated carbon at relatively slow rates over millennia. The apparent L4_C SOC underestimation in these areas may be due to the recent (2000-2013) NRv4 daily climate record used for model SOC initialization; the observed SOC stocks reflect long-term climate conditions.
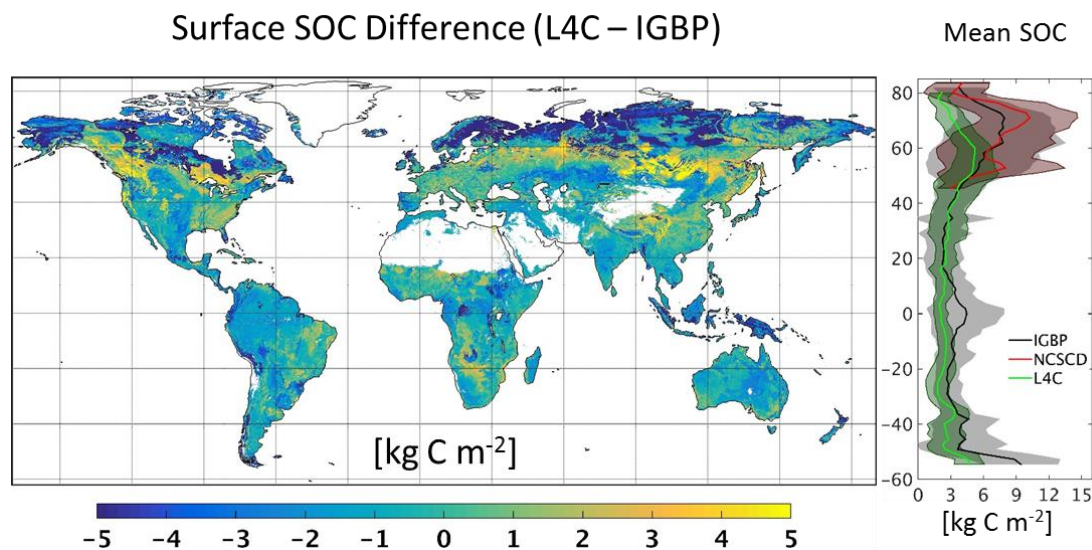


**Figure 7.13**. Difference map between L4_C and IGBP estimated surface SOC stocks (kg C m$^{-2}$). The mean latitudinal SOC distributions and ±1 SD spatial variations (shaded) from the L4_C, IGBP and NCSCD records are also shown.

The L4_C results and IGBP inventory record both show generally lower soil carbon stocks in the temperate and tropical zones, though the L4_C results show lower SOC levels than the IGBP record in the tropics, including the African Congo and portions of tropical Southeast Asia. These relatively low L4_C SOC estimates are due to high estimated soil decomposition and Rh rates in warm, moist tropical climate conditions, with minimal constraints from low soil moisture conditions (e.g. **Fig. 7.2**). The apparent SOC differences may also reflect regional bias in the GEOS-5 land model-derived daily climate inputs used in the L4_C calculations (Yi et al. 2011).

## 7.5  Summary

This report provides an assessment and documentation of the SMAP Level 4 Carbon (L4_C) validated release product.  Methods used to ascertain quality and performance of the L4_C data product included: 1) qualitative evaluations of the product fields for representing expected characteristic spatial and seasonal patterns;  2) comparisons of daily product outputs with tower eddy covariance measurement-based daily carbon ($CO_2$) flux observations from 26 core (CVS) tower sites;  3) comparisons of L4_C daily carbon flux estimates against a larger set of historical tower observations from 228 globally distributed FLUXNET sites; and 4) consistency checks of L4_C product fields against other synergistic global carbon products.  This L4_C validated release assessment exceeds CEOS Stage 1 validation criteria based on a limited set of core validation sites. This assessment also satisfies Stage 2 validation criteria through expanded regional and global assessments involving a diverse set of independent observations. The activities described in this document are also within Stage 3 requirements by including detailed characterization and quantification of product uncertainties in relation to a diverse set of globally representative reference data encompassing a nearly complete annual cycle of SMAP observations.

The primary methods and metrics used for the L4_C Cal/Val assessment included comparisons of collocated time series of *in situ* tower observations and L4_C daily outputs, including net ecosystem $CO_2$ exchange (NEE) and estimated NEE uncertainty (RMSE), and component carbon fluxes for gross primary productivity (GPP) and ecosystem respiration ($R_{eco}$). Comparisons involving CVS sites are both spatially and temporally consistent, while comparisons using the more extensive FLUXNET tower site records are spatially but not temporally consistent as they involve product evaluations against historical tower observations. Other methods employed for the evaluations included comparisons of latitudinal means and spatial patterns between L4_C outputs and other satellite, inventory and model-based observation benchmarks, including the NASA EOS MODIS MOD17 GPP record, the MPI-MTE global tower observation upscaled GPP record, solar-induced canopy fluorescence (SIF) observations from the ESA GOME-2 and NASA OCO-2 satellite sensors, and surface soil organic carbon (SOC) stock estimates from global soil inventory records.

Based on the above assessments, the L4_C validated release product demonstrates a level of performance and accuracy consistent with the algorithm and product design specifications.  The L4_C product shows expected characteristic global patterns and seasonality in estimated carbon fluxes and SOC stocks, with no evidence of obvious artifacts or errors in algorithm performance or formatting. The L4_C global performance assessment indicates that the validated product meets targeted accuracy requirements for NEE (RMSE≤30 g C m$^{-2}$ y$^{-1}$ or 1.6 g C m$^{-2}$ d$^{-1}$) over approximately 66% and 83% of global and northern domains, respectively; these results are consistent with the CVS and global sparse network tower comparisons encompassing almost full year (Apr 2015 – Feb 2016) of observations. The major L4_C product fields also compare favorably with similar variables obtained from a diverse set of global benchmark environmental data records.  The L4_C validated release is suitable for public distribution and utilization by the larger science and application communities.  This validated release effectively replaces an earlier L4_C beta-release product and has suitable performance and accuracy to support scientific investigations and applications. The L4_C product performance and accuracy is expected to improve with continuing SMAP operations, Cal/Val refinements and periodic reprocessing updates.

# 8   OUTLOOK AND FUTURE UPDATES

The L4_C validated release product is relatively mature and exceeds or meets CEOS Stage 1 and Stage 2 (global assessment) validation criteria.  Future product updates and releases are expected based on continuing SMAP operations and further Cal/Val refinements involving a lengthening data record progressing toward multiple years of observations. These activities will continue through all Cal/Val stages over the SMAP mission life span. This report notes several limitations in the current validated release version of the L4_C product, including the use of GEOS-5 surface temperatures rather than SMAP microwave sensor-defined freeze-thaw (FT) constraints on the estimated carbon fluxes. These limitations will be addressed in future L4_C product releases. These future product updates will also include refinements gained from more extensive validation activities involving a longer operational data record and associated calibration improvements to lower order SMAP observation inputs to the L4_C algorithms.  A longer data record will also enable a more comprehensive analysis and quantification of product bias, including systematic and random error components, spatial and seasonal anomalies, and error sources. Elements that will be incorporated into future L4_C product releases include the following:

- *Updated L4_C initialization and calibration.*  The L4_C validated release is based on an initialized model SOC and BPLUT calibration using SMAP L4_SM Nature Run (NRv4) soil moisture inputs, while L4_C operational production uses daily L4_SM inputs derived using the same underlying NRv4 GEOS-5 land model structure (Reichle et al. 2015). Future L4_C product releases will benefit from the latest (NRv5) GEOS-5 land model data and L4_SM inputs.

- *Utilization of SMAP FT inputs.*  The L4_C validated release defines daily frozen temperature controls to ecosystem productivity using relatively coarse resolution GEOS-5 land model-based surface temperatures. This potentially limits the ability of the L4_C product to address SMAP carbon science objectives to quantify frozen temperature constraints to productivity and improve understanding of the boreal carbon sink. Future L4_C product releases will benefit from Cal/Val refinements using SMAP passive microwave sensor-based freeze-thaw (FT) information having enhanced L-band sensitivity to landscape FT dynamics. These activities will enable a more comprehensive assessment and attainment of the SMAP carbon cycle science objectives.

- *Moving toward a Stage 3 validated product.*  The L4_C validated release is limited by a relatively short period (April 2015 – Feb, 2016) of operational assessment. Future product releases will benefit from continuing SMAP operations and refinements spanning multiple years.  With the enhanced inter-comparisons described below, the L4_C validation level should meet CEOS validation Stage 3 criteria in future product releases.

- *Comprehensive product performance assessments.*  Detailed L4_C algorithm sensitivity studies continue to evaluate the global impact of SMAP observations on the model-estimated carbon fluxes. These simulations involve evaluating alternative model simulations derived with and without SMAP observation-informed inputs, including FT and SM inputs, and their individual and combined impacts. Continuing efforts will clarify the improved assessment and understanding gained through the SMAP observations on the estimated L4_C product variables spanning a global domain and one or more complete annual cycles of SMAP observations. These simulations will also incorporate the latest Cal/Val refinements and updates to lower order (L3 and L4) inputs, enabling a more robust assessment of SMAP science impacts.

- *Refined CVS assessment.*  The methodology and outcome of the CVS comparisons used in the L4_C validated release assessment is relatively mature, but was limited to less than 1 year of observations. Planned CVS assessments may include a longer set of tower observations spanning one or more complete annual cycles and a larger set of participating CVS towers. The tower observation uncertainty is expected to be better characterized and incorporated into future L4_C validation assessments.

- *More extensive satellite data comparisons.* A variety of global carbon products have been used as benchmarks for evaluating the general quality and performance of the L4_C validated release. Future activities will include the use of longer observational data records spanning one or more annual cycles and benefiting from continuing refinements and product updates in these other benchmark observations, including OCO-2.

- *Incorporating Field Campaign datasets for algorithm assessment and refinement.* A SMAP validation field campaign will be conducted in mid-2016 (SMAPVEX16), while another major field experiment and airborne campaign will begin in 2016 as part of the NASA Arctic Boreal Vulnerability Experiment (ABoVE). Future L4_C product releases will benefit from Cal/Val assessments and refinements enabled by these new data collections.

# 9 ACKNOWLEDGEMENTS

# 10 REFERENCES

Baccini, A., S.J. Goetz, W.S. Walker, et al., 2012. Estimated carbon dioxide emissions from tropical deforestation improved by carbon-density maps. *Nature Climate Change* 2, 182-185.

Baldocchi, D., 2008: Breathing of the terrestrial biosphere: lessons learned from a global network of carbon dioxide flux measurement systems. *Austr. J. Bot.*, 56: 1-26.

Du, J., J.S. Kimball, M. Azarderakhsh, R.S. Dunbar, M. Moghaddam, and K.C. McDonald, 2015. Classification of Alaska spring thaw characteristics using satellite L-band Radar remote sensing. *IEEE Transactions on Geoscience and Remote Sensing* 53 (1), 542-556.

Entekhabi, D., E.G. Njoku, P.E. O'Neill, et al., 2010. The Soil Moisture Active and Passive (SMAP) Mission. *Proceedings of the IEEE* 98 (5), 704-716.

Entekhabi, D., S. Yueh, P. O'Neill, K. Kellogg et al., SMAP Handbook, JPL Publication, JPL 400-1567, Jet Propulsion Laboratory, Pasadena, California, 182 pages, 2014. https://smap.jpl.nasa.gov/files/smap2/SMAP_Handbook_FINAL_1_JULY_2014_Web.pdf.

Frankenberg, C., C. O'Dell, J. Berry, L. Guanter, J. Joiner, P. Köhler, R. Pollock, and T.E. Taylor, 2014. Prospects for chlorophyll fluorescence remote sensing from the Orbiting Carbon Observatory-2. *Remote Sensing of Environment* 147, 1-12.

Glassy, J., J.S. Kimball, R.H. Reichle, J.V. Ardizzone, G-K. Kim, R.A. Lucchesi, and B.H. Weiss, 2015. Soil Moisture Active Passive (SMAP) Mission Level 4 Carbon (L4_C) Product Specification Document. GMAO Office Note No. 12 (Version 1.9), 71 pp, NASA Goddard Space Flight Center, Greenbelt, MD, USA. Available from http://gmao.gsfc.nasa.gov/pubs/office_notes.

Guanter, L., Y. Zhang, M. Jung, et al. 2013. Global and time-resolved monitoring of crop photosynthesis with chlorophyll fluorescence. *PNAS* 111, 14, E1327-E1333.

Global Soil Data Task Group. 2000. Global Gridded Surfaces of Selected Soil Characteristics (IGBP-DIS). [Global Gridded Surfaces of Selected Soil Characteristics (International Geosphere-Biosphere Programme - Data and Information System)]. Data set. Available on-line [http://www.daac.ornl.gov] from Oak Ridge National Laboratory Distributed Active Archive Center, Oak Ridge, Tennessee, U.S.A. doi:10.3334/ORNLDAAC/569.

Hugelius, G., J. Strauss, S. Zubrzycki, et al., 2014. Estimated stocks of circumpolar permafrost carbon with quantified uncertainty ranges and identified data gaps. *Biogeosciences* 11, 6573-6593.

Jackson, T., A. Colliander, J. Kimball, R. Reichle, W. Crow, D. Entekhabi, P. O'Neill, and E. Njoku, 2014. SMAP Science Data Calibration and Validation Plan. SMAP Project, JPL D-52544, Jet Propulsion Laboratory, Pasadena CA, 96 pp (http://smap.jpl.nasa.gov/files/smap2/CalVal_Plan_120706_pub.pdf).

Jobbagy, E. G., & R. B. Jackson. 2000. The vertical distribution of soil organic carbon and its relation to climate and vegetation. *Ecol. Applications*, 10 (2): pp. 423-36.

Joiner, J., L. Gaunter, R. Lindstrot, et al., 2013. Global monitoring of terrestrial chlorophyll fluorescence from moderate-spectral-resolution near-infrared satellite measurements: methodology, simulations, and application to GOME-2. *Atmos. Meas. Tech.*, 6, 2803-2823.

Jung, M., M. Reichstein, H.A. Margolis, et al., 2011. Global patterns of land-atmosphere fluxes of carbon dioxide, latent heat, and sensible heat derived from eddy covariance, satellite, and meteorological observations. *J. Geophys. Res. Biogeosci*. 116, G3, DOI:10.1029/2010JG001566.

Kimball, J.S., L.A. Jones, J.P. Glassy, and R. Reichle, 2014. SMAP Algorithm Theoretical Basis Document, Release A: L4 Carbon Product. SMAP Project, JPL D-66484, Jet Propulsion Laboratory, Pasadena CA., 76 pp, (http://smap-archive.jpl.nasa.gov/files/smap2/L4_C_RevA.pdf).

Kimball, John S., Lucas A. Jones,Joseph Glassy, E. Natasha Stavros, Nima Madani, Rolf H. Reichle, Thomas Jackson, and Andreas Colliander, 2015. Soil Moisture Active Passive (SMAP) Project Calibration and Validation for the L4_C Beta-Release Data Product. *NASA/TM–2015-104606*, Vol. 42, 37 pp. Document (13765 kB).

Madani, N., J.S. Kimball, D.L.R. Affleck, J. Kattge, J. Graham, P.M. van Bodegom, P.B. Reich, and S.W. Running, 2014. Improving ecosystem productivity modeling through spatially explicit estimation of optimal light use efficiency. *J. Geophys. Res. Biogeosci.*, 119, 9, 1755-1769.

Peters, W. et al. (2007), An atmospheric perspective on North American carbon dioxide exchange: CarbonTracker, PNAS, November 27, 2007 , vol. 104, no. 48, 18925-18930.

Podest, E., K.C. McDonald, and J.S. Kimball, 2014. Multisensor microwave sensitivity to freeze/thaw dynamics across a complex boreal landscape. *IEEE TGARS* 52, 11.

Porcar-Castell, A., E. Tyystjarvi, J. Atherton, et al., 2014. Linking chlorophyll a fluorescence to photosynthesis for remote sensing applications: mechanisms and challenges. *Journal of Experimental Botany* 66, 19, doi:101093/jxb/eru191.

Reichle, R.H., G.J.M. De Lannoy, Q. Liu, A. Colliander, A. Conaty, T. Jackson, J. Kimball, and R.D. Koster, 2015. *Soil Moisture Active Passive (SMAP) Project Assessment Report for the Beta-Release L4_SM Data Product*. *NASA/TM-2015-104606*, Vol. **40**. Document (5812 kB).

Schimel, D., R. Pavlick, J.B. Fisher, et al. 2015. Observing terrestrial ecosystems and the carbon cycle from space. *Global Change Biology* 21, 1762-1776.

Turner, D.P., W.D. Ritts, W.B. Cohen, et al. 2006. Evaluation of MODIS NPP and GPP products across multiple biomes. *Remote Sensing of Environment*, 102, 3-4, 282-292.

Yi, Y., J.S. Kimball, L.A. Jones, R.H. Reichle and K.C. McDonald, 2011. Evaluation of MERRA land surface estimates in preparation for the Soil Moisture Active Passive Mission. *Journal of Climate* 24(15), 3797-3816.

Yi, Y., J.S. Kimball, L.A. Jones, R.H. Reichle, R. Nemani, and H.A. Margolis, 2013. Recent climate and fire disturbance impacts on boreal and arctic ecosystem productivity estimated using a satellite-based terrestrial carbon flux model. *J. Geophys. Res*. *Biogeosci*. 118, 1-17.

Zhao, M., and S.W. Running, 2010. Drought-induced reduction in global terrestrial net primary production from 2000 through 2009. *Science* 329, 5994, 940-943.